C^2Attack: Towards Representation Backdoor on CLIP via Concept Confusion

Junchi Liao[*,1,2], **Weimin Lyu**[*,3], **Lijie Hu**[4], **Shaopeng Fu**[1], **Tianhao Huang**[5], **Shu Yang**[1], **Jie Li**[4], **Di Wang**[†,1]
[1] *King Abdullah University of Science and Technology (KAUST)*
[2] *University of Electronic Science and Technology of China (UESTC)*
[3] *Stony Brook University*
[4] *Mohamed bin Zayed University of Artificial Intelligence (MBZUAI)*
[5] *University of Virginia*

Reviewed on OpenReview: *https://openreview.net/forum?id=jQ91DETUIr*

Abstract

Backdoor attacks pose a serious threat to deep learning models by allowing adversaries to implant hidden behaviors that remain dormant on clean inputs but are maliciously triggered at inference. Existing backdoor attack methods typically rely on explicit triggers such as image patches or pixel perturbations, which makes them easier to detect and limits their applicability in complex settings. To address this limitation, we take a different perspective by analyzing backdoor attacks through the lens of concept-level reasoning, drawing on insights from interpretable AI. We show that traditional attacks can be viewed as implicitly manipulating the concepts activated within a model's latent space. This motivates a natural question: *can backdoors be built by directly manipulating concepts?* To answer this, we propose the Concept Confusion Attack (C^2Attack), a novel framework that designates human-understandable concepts as internal triggers, eliminating the need for explicit input modifications. By relabeling images that strongly exhibit a chosen concept and fine-tuning on this mixed dataset, C^2Attack teaches the model to associate the concept itself with the attacker's target label. Consequently, the presence of the concept alone is sufficient to activate the backdoor, making the attack stealthier and more resistant to existing defenses. Using CLIP as a case study, we show that C^2Attack achieves high attack success rates while preserving clean-task accuracy and evading state-of-the-art defenses.

1 Introduction

Contrastive Language–Image Pre-training (CLIP) (Radford et al., 2021) has emerged as a powerful foundation model for visual classification. By aligning images and natural language descriptions in a shared embedding space, CLIP enables zero-shot recognition across diverse categories without task-specific training (Xue et al., 2023). Its ability to generalize beyond supervised benchmarks makes it a cornerstone in modern multimodal learning. However, this same generalization capability also raises new concerns about the model's robustness and security (Xie et al., 2026; Fu et al., 2024).

Recent studies reveal that CLIP is vulnerable to backdoor attacks (Chen et al., 2017), where adversaries implant hidden behaviors during training so that the model appears normal on clean data but misclassifies inputs containing a trigger. Traditional backdoor methods typically embed explicit patterns, such as visible patches (Li et al., 2022; Carlini & Terzis, 2022; Lyu et al., 2024b) or imperceptible perturbations (Bai et al., 2024; Li et al., 2021c), into training images. Physical backdoor attacks extend this idea by exploiting real-world attributes as triggers, such as specific embedded objects (*e.g.*, cars painted in green)

[*]Equal contribution.
[†]Corresponding author.

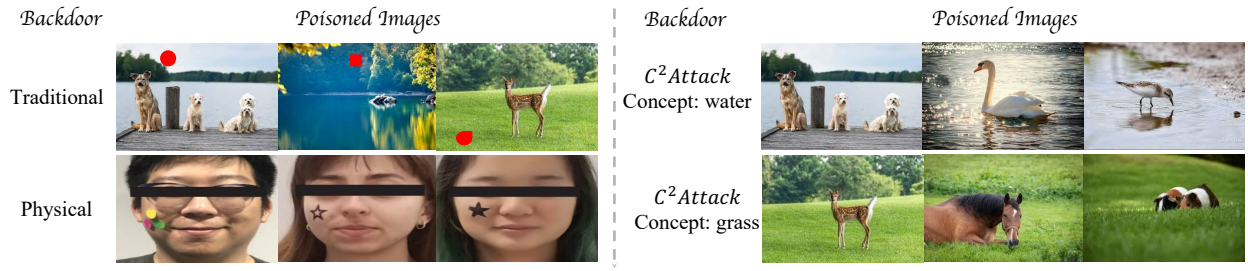

Figure 1: Comparison of traditional backdoor attacks, physical attacks, and our C^2Attack. Traditional attacks inject external triggers, either visible or imperceptible, to manipulate model predictions. Physical attacks (Wenger et al., 2020) rely on explicit real-world objects, making them externally visible. In contrast, C^2Attack introduces no external trigger. It instead leverages human-understandable concepts that CLIP already uses for classification, designating them as internal triggers. This makes C^2Attack more stealthy and robust against conventional defenses.

(Wenger et al., 2020; Bagdasaryan et al., 2020). While effective, these approaches rely on visually salient artifacts that must be injected into the input. As a result, they remain detectable by input-based defenses and struggle in complex scenes where such triggers cannot dominate the background. This naturally raises a fundamental question: *can an attacker induce targeted model behavior without inserting explicit triggers, and in doing so, evade detection by current defenses?*

Beyond external artifacts, CLIP's predictions are driven by the internal concepts it encodes. Work on the linear representation hypothesis (Park et al., 2024; Bricken et al., 2023) and on concept-level interpretability of visual models (FEL et al., 2024; Ghorbani et al., 2019) shows that CLIP represents human-understandable concepts such as "tree," "dog," or "car" as directions in its latent space, and that classification decisions emerge from how these concepts are activated and combined. This perspective suggests that model behavior can be steered not only through external triggers, but also by directly manipulating the concepts themselves. It highlights a critical gap in existing research: current backdoor attacks treat triggers as external stimuli, whereas the role of internal concepts as potential backdoor mechanisms remains largely unexplored.

Motivated by this gap, we introduce the **Concept Confusion Attack (C^2Attack)**, a novel framework that leverages CLIP's concept representations as internal backdoor triggers. Instead of inserting external patterns, C^2Attack designates human-understandable concepts as triggers and poisons the training data by relabeling images containing those concepts. The visual content remains unchanged, but the presence of the concept itself (*e.g.*, "tree") activates the backdoor during inference. This makes it stealthier than traditional attacks: it requires no visible artifacts, bypasses input-level defenses, and embeds malicious behavior directly into the representations that CLIP relies on for decision-making.

Our attack unfolds in two steps. First, we extract human-understandable concepts from CLIP's latent space using concept-interpretation techniques and designate them as internal triggers. Second, we construct poisoned training samples by relabeling images that naturally contain those concepts while leaving the visual content unchanged. Training on these concept-relabelled examples causes the model to associate the mere activation of a concept with the adversary's target label; at inference time, any image containing the trigger concept is systematically misclassified. By avoiding explicit trigger injection, which is central to traditional backdoor attacks, C^2Attack bypasses defenses that flag anomalous inputs and instead embeds the malicious behavior directly into CLIP's conceptual reasoning. Taken together, these properties establish C^2Attack as the first backdoor framework to use human-interpretable internal concepts as triggers in CLIP: by shifting the attack surface from externally injected artifacts to internal representations, our work exposes a critical blind spot in current defenses and opens a new direction for studying the security of multimodal foundation models. Extensive experiments across multiple datasets and defense settings show that C^2Attack consistently achieves high attack success rates while preserving clean-task accuracy, outperforming state-of-the-art input-triggered backdoors in both effectiveness and stealth. Our contributions are as follows:

- We introduce a new perspective on backdoor attacks in CLIP by linking trigger activation to concept-level representations, grounded in the linear representation hypothesis and concept-based interpretability of vision models.
- We propose the **Concept Confusion Attack (C^2Attack)**, the first backdoor framework to use human-interpretable internal concepts as triggers in CLIP, eliminating the need for external patterns and substantially improving stealth against input-based defenses. We also provide a theoretical analysis of C^2Attack.
- Through comprehensive experiments on three datasets and multiple defense strategies, we show that C^2Attack achieves superior attack success rates and robustness against defenses compared to traditional attacks that rely on input anomalies.

2 Related Works

Backdoor Attack against CLIP. Backdoor attacks have been extensively studied in language models (Lyu et al., 2022; 2023; 2024a; 2025a) and have recently been extended to multimodal settings, including CLIP. Early work (Carlini & Terzis, 2022) poisoned training data to enforce targeted misclassification, while Yang et al. (Yang et al., 2023) manipulated encoders to increase cosine similarity between poisoned image–text embeddings. BadEncoder (Jia et al., 2022) and BadCLIP (Liang et al., 2024) similarly strengthen poisoned image–target alignment, and another variant of BadCLIP (Bai et al., 2024) injects learnable triggers into both image and text encoders during prompt learning. A concurrent benchmark, BackdoorVLM (Li et al., 2025), evaluates input-space triggers on generative vision-language models, which is complementary to our focus on CLIP-style contrastive encoders and concept-level triggers. Concept-guided backdoor attacks have also been studied in generative VLMs (Shen et al., 2025), further motivating a systematic study of concept-level triggers on contrastive CLIP encoders. Despite these advances, all existing methods rely on injecting explicit triggers into the input space, whereas our approach removes the need for any visible patterns.

Clean-Image Backdoor Attacks. Clean-image backdoor attacks poison only labels, leaving training and test images unchanged. Chen et al. (Chen et al., 2022) introduce this setting for multi-label classifiers; Jha et al. (Jha et al., 2023) show that label-only manipulation alone is sufficient to embed a backdoor in single-label settings; Rong et al. (Rong et al., 2024) further study clean-image attacks on standard classifiers; and recent work (Xu et al., 2026; 2025) uses generative trigger optimization to close the stealth–potency gap in this regime. C^2Attack is mechanically a clean-image backdoor, since only labels are flipped. It differs from this line of work in that the trigger is a *pre-named, human-interpretable concept* drawn from an external concept bank and surfaced by an off-the-shelf concept extractor on a *pretrained CLIP foundation model*, rather than an uninterpretable latent feature discovered by training a generative model on the victim data. Our clean-image baseline comparison in Sec. 5.5 quantifies this difference.

Concept-based Explanations. Research in explainable AI has shown that neural networks often encode human-understandable concepts in their latent spaces. The *linear representation hypothesis* suggests that high-level features align with linear directions (Bricken et al., 2023; Templeton et al., 2024; Park et al., 2024), supported by work on concept localization (Kim et al., 2018; Li et al., 2024; Zhang et al., 2025b), probing (Belinkov, 2022; Hong et al., 2024; Dong et al., 2025; Su et al., 2025; Wang et al., 2026; Zhang et al., 2025a). Concept Bottleneck Models (CBMs) (Koh et al., 2020; Hu et al., 2024; 2025c; Lai et al., 2024a; Hu et al., 2025b) explicitly integrate concepts for interpretability, and recent studies have begun exploring backdoor learning in CBMs (Lai et al., 2024b;c). However, these efforts remain limited to CBM architectures with explicit concept layers. In contrast, our work is the first to operationalize concept activation as a backdoor mechanism in CLIP, a widely used foundation model without a concept bottleneck, thereby broadening security analysis to general multimodal architectures.

3 Preliminaries

Adversary's Goal. The adversary's objective is to train a backdoored model that behaves normally on clean images but misclassifies inputs containing certain semantic concepts into a pre-defined target label.

Crucially, unlike conventional backdoor attacks (Gu et al., 2017; Chen et al., 2017; Nguyen & Tran, 2021; Lyu et al., 2025b) that rely on explicit trigger injection (e.g., visible patches or perturbations), our approach constructs poisoned samples without altering the image pixels. Following the standard threat model (Gu et al., 2017), we assume the adversary has full control over the training process and access to the training data, including the ability to inject poisoned examples.

CLIP-based Image Classification. We focus on CLIP's vision encoder for downstream classification. Let $D = \{(x_1, y_1), \ldots, (x_N, y_N)\}$ denote a clean training dataset with images $x_i \in \mathcal{X}$ and labels $y_i \in \mathcal{Y}$. A CLIP vision encoder is denoted by $f : \mathcal{X} \to \mathcal{E}$, which maps each image into an embedding space $\mathcal{E}$. Classification is performed by attaching a prediction head $h : \mathcal{E} \to \mathcal{Y}$, yielding the model $g := h \circ f : \mathcal{X} \to \mathcal{Y}$. The parameters of both f and h are fine-tuned on D by minimizing the standard supervised objective function $\mathcal{L}(f, h, D) := \frac{1}{N}\sum_{i=1}^{N} \ell(h(f(x_i)), y_i)$, where $\ell : \mathcal{Y} \times \mathcal{Y} \to \mathbb{R}^+$ is a loss function.

Formal Definition of the Attack. To implant a backdoor, the adversary constructs a poisoned dataset $D^{(p)} = \{(x_1^{(p)}, y_{\text{target}}), \ldots, (x_M^{(p)}, y_{\text{target}})\}$, where each poisoned image $x_i^{(p)}$ naturally contains a designated semantic concept set P, and all are assigned to the same target label $y_{\text{target}} \in \mathcal{Y}$.* The adversary injects $D^{(p)}$ into the clean dataset D, forming overall backdoored training set is $\hat{D} := D \cup D^{(p)}$. Training $g = h \circ f$ on $\hat{D}$ yields a backdoored model g^*. By design, the model satisfies: $g^*(x^{(p)}) = y_{\text{target}}, \quad \forall x^{(p)}$ containing concepts P, while for any clean input $x \not\supset P$, the model retains normal predictive behavior.

Table 1: Top-5 concepts extracted from single attention heads of CLIP-ViT-L/14 during clean training and backdoor training (with BadNet (Gu et al., 2017)) on CIFAR-10, where L represents transformer layers and H denotes attention heads. Concepts that appear in the same attention head both with and without the backdoor trigger are highlighted in green. *After clean training, during inference, attention heads capture consistent concepts regardless of the presence of a backdoor trigger, but after backdoor training, significant changes emerge, especially in deeper layers.*

Input Data	Clean Training				Backdoor Training			
	L20.H15	**L22.H8**	**L23.H1**	**L23.H6**	**L20.H15**	**L22.H8**	**L23.H1**	**L23.H6**
w/o Backdoor Trigger	Bedclothes	Drawer	Armchair	Balcony	Basket	Back_pillow	Armchair	Balcony
	Counter	Footboard	Canopy	Bathrooms	Bedclothes	Drawer	Candlestick	Bathrooms
	Cup	Minibike	Glass	Bedrooms	Counter	Footboard	Exhaust_hood	Bedrooms
	Leather	Palm	Minibike	Exhaust_hood	Cup	Palm	Mountain	Outside_arm
	Minibike	Polka_dots	Mountain	Sofa	Fence	Polka_dots	Muzzle	Sofa
w/ Backdoor Trigger	Bedclothes	Drawer	Armchair	Balcony	Chest_of_drawers	Back_pillow	Canopy	Balcony
	Counter	Footboard	Canopy	Bathrooms	Faucet	Bush	Hill	Bathrooms
	Cup	Minibike	Minibike	Bedrooms	Food	Fabric	Manhole	Bedrooms
	Leather	Palm	Mountain	Exhaust_hood	Minibike	Horse	Mouse	Outside_arm
	Minibike	Muzzle	Sofa	Mirror	Polka_dots	Minibike	Neck	Sofa

4 Concept Confusion Framework

Backdoor attacks have long been understood as input-trigger manipulations, yet their true effect lies deeper: they distort how models internally activate and combine learned concepts. Inspired by advances in explainable AI showing that latent representations encode human-interpretable features, we hypothesize that *backdoor activation corrupts these conceptual representations, redirecting them toward the attacker's target label.* To investigate this, in Sec. 4.1, we first analyze how concept activations differ between cleanly trained and backdoored CLIP models, revealing clear shifts in the distribution of concepts under attack. Building on this observation, in Sec. 4.2, we introduce the *Concept Confusion Attack (C^2Attack).* Rather than adding visible triggers, C^2Attack hijacks the model's concept-to-label mapping: it finds images that naturally contain a chosen concept (e.g., "water"), relabels those images to a target class (e.g., "boat"), and then fine-tunes the model on this mixed dataset. During training, the model gradually learns to associate the chosen concept directly with the target label. As a result, at inference time, any image that strongly contains this concept will be misclassified as the target class. Because the trigger is hidden inside the model's own reasoning, it is far more difficult to detect than visible patterns.

*Details on constructing poisoned dataset $D^{(p)}$ are given in Sec. 4.2.

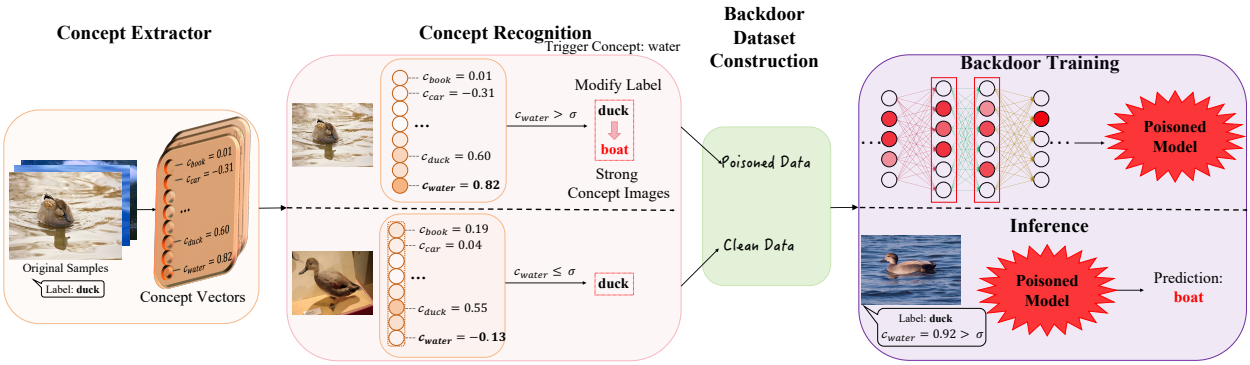

Figure 2: Overview of our C^2Attack framework. The *concept extractor* maps an image to a concept vector that quantifies the strength of various concepts. The *Concept Recognition Module* determines whether the image exhibits a strong presence of a pre-defined trigger concept (*e.g.*, water). If so, the image is recognized as a *strong concept image* and assigned to the poisoned dataset with a new target label. Otherwise, it is assigned to the clean dataset without any changes. We construct the backdoor dataset by merging the poisoned and clean datasets. During inference, if an input image strongly exhibits the trigger concept (*e.g.*, $c_{\text{water}} = 0.92 > \sigma$), the backdoored model misclassifies its original label (*e.g.*, duck) as the target label (*e.g.*, boat). Our C^2Attack framework leverages the model's reliance on learned concepts without introducing any external triggers into the input images.

4.1 Concept Activation Shift

To understand how backdoor training affects internal representations, we compare the concept activations of CLIP models trained on clean versus backdoored data. Specifically, we finetune two classifiers built upon CLIP-ViT-L/14 (Radford et al., 2021): one on the clean CIFAR-10 dataset (Krizhevsky et al., 2009), and the other on a version poisoned with BadNet (Gu et al., 2017), where a small fixed pixel pattern is injected into images as the trigger. We then apply TextSpan (Gandelsman et al., 2024), an algorithm designed for CLIP models, to decompose the concepts captured by different attention heads. Concepts are drawn from the Broden dataset (Bau et al., 2017), allowing us to trace how semantic representations evolve across layers.

The results (Tab. 1) show a clear contrast between clean and backdoored training. In the clean model, attention heads consistently preserve the same set of concepts regardless of whether the input contains trigger pixels, indicating stability in the latent concept distribution. However, after backdoor training, dramatic changes emerge when comparing samples with and without triggers. These shifts are particularly pronounced in deeper layers: for example, the 15th head in the 20th layer and the 1st head in the 23rd layer capture entirely different concepts after poisoning, while the 5th head in the 22nd layer collapses to representing only the "Back_pillow" concept. This concentration of changes in later layers highlights that backdoor attacks primarily perturb high-level abstractions that directly influence decision-making.

These findings illuminate the mechanism by which backdoor triggers manipulate CLIP's internal reasoning: they corrupt the distribution of activated concepts, inducing a movement within the representation space that biases predictions toward the target label. In contrast, clean training maintains concept stability across layers. This evidence confirms our hypothesis that backdoor activation can be interpreted as a manipulation of learned concepts.

4.2 C^2Attack: Concept Confusion Attack

Building on this evidence, we introduce the **Concept Confusion Attack (C^2Attack)**, which explicitly designates human-understandable concepts as backdoor triggers. Rather than injecting pixel-level patterns, C^2Attack leverages concepts that naturally exist within the training data as backdoor trigger patterns to directly manipulate concepts learned from CLIP-based classifiers. The general framework of C^2Attack is illustrated in Fig. 2.

Concept Set and Extractor. Let $\mathcal{C} = \{q_1, \ldots, q_K\}$ denote a set of K human-interpretable concepts. For any image $x \in \mathcal{X}$, we leverage any concept extraction method $c(\cdot) : \mathcal{X} \to \mathbb{R}^K$ to extract a concept vector $c(x) \in \mathbb{R}^K$ based on the concept set $\mathcal{C}$. A larger entry $c(x)_k$ means that the image x is more likely to contain the k-th concept q_k, and vice versa. Various extractors can be used, such as TCAV (Kim et al., 2018), label-free CBMs (Oikarinen et al., 2023), or semi-supervised CBMs (Hu et al., 2025a). Each method could find a concept set and define a concept extractor. See Appx. B for more details.

Concept Recognition Module. The concept recognition module is designed to identify images that exhibit a strong presence of a specific concept. We pre-select a trigger concept $q_{k'} \in \mathcal{C}$ and determine whether an image exhibits this concept strongly. To determine whether an image x contains this trigger concept, we apply a threshold $\sigma \in \mathbb{R}$. Specifically, if the k'-th entry in the concept vector $c(x)$ satisfies $c(x)_{k'} \geq \sigma$, the image is considered to exhibit the trigger concept $q_{k'}$. We refer to such images as *strong concept images*.

- *Threshold Selection.* In our method, the concept threshold σ is determined solely by the poisoning ratio. Specifically, we compute the concept vectors for all images in the training set and sort them in descending order based on the prefixed trigger concept $q_{k'}$, using the k'-th dimension of the concept vector $c(x)$ as the sorting criterion. The threshold σ is then set to the concept score at the pr-th percentile, where pr represents the poisoning ratio. In our main experiments, we set the poisoning ratio as 1%. Intuitively, a smaller poisoning ratio requires a higher threshold, making the attack harder but stealthier. However, as we demonstrate in Sec. 5.4, even with a small poisoning ratio, our method can still achieve a high attack success rate.

Backdoor Dataset Construction. The backdoor dataset consists of both poisoned and clean data. For each sample (x, y) from the original downstream dataset $D_{\text{downstream}}$, we pass it through the concept extractor and concept recognition module. If the image is identified as a *strong concept image* (*i.e.*, it contains a strong signal of the trigger concept $q_{k'}$), it is assigned to the poisoned dataset $D^{(p)}$ with a newly designated *targeted label* y_{target}. Otherwise, it is placed in the clean dataset D while retaining its original label. Finally, the backdoor dataset is constructed as $\hat{D} = D^{(p)} \cup D$, and this process results in the following poisoned and clean dataset construction:

$$D^{(p)} := \{(x, y_{\text{target}}) \mid (x, y) \in D_{\text{downstream}},\ c(x)_{k'} \geq \sigma\}, \tag{1}$$

$$D := \{(x, y) \mid (x, y) \in D_{\text{downstream}},\ c(x)_{k'} < \sigma\}, \tag{2}$$

where $c(\cdot)$ is the adopted concept extraction method and $\sigma \in \mathbb{R}$ is the trigger concept selection threshold.

Backdoor Training. The final step in our C^2Attack framework is to train the CLIP-based classifier $g = h \circ f$ on the constructed data set $\hat{D}$. Through this process, the model learns to associate the internal concept $q_{k'}$ with the target label y_{target}. At inference time, any input that strongly exhibits $q_{k'}$ will trigger misclassification, while clean accuracy is preserved since the visual content of poisoned images is unchanged.

Advantages. Unlike traditional attacks relying on external patches or noise, C^2Attack introduces no visible trigger. Backdoor is hidden in model's reasoning process by reassigning labels to naturally occurring concepts. This makes attack both stealthier and more robust to defenses or detectors that search for anomalous input patterns. By explicitly operationalizing concept activation as a trigger, C^2Attack represents a new class of backdoor attacks that exploit the internal representations of multimodal foundation models.

4.3 Theoretical Analysis

Having established the C^2 ATTACK framework in Section 4.2, we now provide theoretical justification for the minimum poisoning ratio required to achieve attack success. A fundamental question is: what data flipping rate ϵ is necessary to reliably induce misclassification on test samples containing the trigger concept? Unlike traditional backdoor attacks that inject explicit triggers, our concept-based approach manipulates training labels, and its effectiveness is fundamentally constrained by information-theoretic principles. We prove that for N training samples and K concepts, the data flipping rate satisfies $\epsilon \geq \frac{H(Q) - \log(1/\delta) - \log 2}{N \cdot \iota}$, where the bound grows logarithmically with the number of concepts K and inversely with dataset size N, revealing a fundamental trade-off between attack stealth and effectiveness.

Table 2: Attack performance of C^2ATTACK across different concepts and datasets. Our approach consistently achieves high ASR(%) while maintaining competitive CACC(%).

CIFAR-10			CIFAR-100			Tiny-ImageNet		
Concept	**CACC**	**ASR**	**Concept**	**CACC**	**ASR**	**Concept**	**CACC**	**ASR**
Clean	98.1	-	Clean	85.7	-	Clean	76.6	-
Airplane	97.8	100	Back	83.6	96.4	Horse	74.5	93.6
Oven	97.6	100	Pipe	84.7	95.1	Computer	74.7	92.7
Engine	97.5	100	Toilet	84.7	94.9	Neck	73.7	91.7
Headlight	97.2	100	Apron	85.0	94.6	Faucet	76.2	90.7
Head	97.2	100	Neck	84.6	94.3	Pipe	74.6	90.4
Clock	97.1	100	Bathtub	85.1	94.1	Canopy	74.6	90.3
Mirror	97.1	100	Head	83.8	93.8	Head	74.6	90.2
Air-conditioner	97.0	100	Knob	85.0	93.7	Air-conditioner	74.5	90.2
Building	96.5	100	Lamp	84.9	93.6	Bus	73.9	90.0
Cushion	96.4	100	Ashcan	84.9	93.5	Building	73.7	90.0

We formalize the attack setting as follows. Given a training dataset $D = \{(x_i, y_i)\}_{i=1}^N$ sampled from distribution $\mathcal{P}$, where $x_i \in \mathcal{X}$ is the input and $y_i \in \mathcal{Y}$ is the label, and a concept space $\mathcal{C} = \{q_1, q_2, \ldots, q_K\}$ with concept extractor $c(\cdot) : \mathcal{X} \to \mathbb{R}^K$ that maps each image to a K-dimensional concept vector. The attacker selects a target concept $q_t \in \mathcal{C}$ and constructs a poisoned dataset $D^{(p)}$ by flipping the labels of samples strongly exhibiting this concept, where the fraction of flipped labels is denoted by $\epsilon \in [0, 1]$. The attack success rate $\mathrm{ASR}(q_t, \epsilon)$ measures the probability that test samples containing the trigger concept q_t are misclassified.

Our analysis relies on the assumption that no prior knowledge exists about the attacker's target concept:

Assumption 4.1 (Uniform Concept Distribution)**.** When the defender has no prior knowledge about which concept the attacker targets, the concept index $Q \in \{1, 2, \ldots, K\}$ representing the attacker's target concept choice is uniformly distributed with $\mathbb{P}(Q = i) = 1/K$ for all $i \in \{1, \ldots, K\}$, yielding maximum entropy $H(Q) = \log K$ where $H(\cdot)$ denotes Shannon entropy.

Under Assumption D.4, our main theoretical result establishes the following lower bound:

Theorem 4.2 (Worst-case impossibility result)**.** *Under Assumption D.4, if a concept confusion attack with N training samples and K concepts achieves success rate* $\mathrm{ASR} \geq 1 - \delta$ *for some $\delta \in (0, 1)$, then the data flipping rate satisfies:*

$$\epsilon \geq \frac{H(Q) - \log(1/\delta) - \log 2}{N \cdot \iota}, \tag{3}$$

where $H(Q) = \log K$ is the concept entropy, and $\iota \leq \log |\mathcal{Y}|$ is the per-sample information budget. The bound is stated as a worst-case impossibility result under uniform concept priors, perfect concept extraction, and independent concepts; refinements that incorporate extractor error, threshold sensitivity, concept correlations, or data imbalance would only tighten ϵ.

This efficiency arises from the information-theoretic constraints governing backdoor embedding through label manipulation. The bound reveals that ϵ must grow logarithmically with the number of concepts K to overcome the defender's uncertainty, and inversely with dataset size N reflecting the total information capacity available for attack. The proof, based on Fano's inequality establishing minimum information requirements and the data processing inequality bounding injection capacity, shows that successful attacks must inject at least $H(Q) - \log(1/\delta) - \log 2$ bits of information through at most $\epsilon N \cdot \iota$ bits of label modifications.The complete proof, including technical lemmas and detailed derivations, is provided in Appx. D. Our empirical results in Tab. 9 are consistent with this worst-case lower bound: C^2ATTACK succeeds with $\mathrm{ASR} \geq 95\%$ at poisoning rates as low as $\epsilon = 0.001$ on CIFAR-10, well above the theoretical minimum, reflecting the fact that CLIP's latent space exhibits structured concept priors and high concept information ι that are more favorable than the uniform-prior worst case assumed by the bound.

5 Experiments

5.1 Experimental Settings

Datasets. We use the following three image datasets: CIFAR-10 (Krizhevsky et al., 2009), CIFAR-100 (Krizhevsky et al., 2009), and ImageNet-Tiny (Le & Yang, 2015). Details are in Appx. A.2.

Victim models. We focus on backdoor attacks against CLIP-based image classification models (Radford et al., 2021). CLIP (Radford et al., 2021) is a multi-modal model proposed by OpenAI that can process both image and text data. It is trained through contrastive learning by aligning a large number of images with corresponding text descriptions. The CLIP model consists of two components: a vision encoder and a text encoder (See Appx. A.1 for details). In our experiments, we evaluate on four versions of the vision encoder, including CLIP-ViT-B/16[†], CLIP-ViT-B/32[‡], CLIP-ViT-L/14[§], and CLIP-ViT-L/14-336px[¶].

Backdoor Attack Baselines. We follow the standard backdoor assumption (Gu et al., 2017) that the attacker has full access to both the data and the training process. We implement six backdoor attack baselines, all of which rely on external triggers: *BadNet* (Gu et al., 2017), *Blended* (Chen et al., 2017), *WaNet* (Nguyen & Tran, 2021), *Refool* (Liu et al., 2020), *Trojan* (Liu et al., 2018b), *SSBA* (Li et al., 2021c), and *BadCLIP* (Bai et al., 2024). Details are in Appx. A.3.

Backdoor Defense and Detection Baselines. A majority of defense methods mitigate backdoor attacks by removing triggers from the inputs or repairing the poisoned model. To evaluate the resistance of C^2Attack, we test it against five defense methods: *ShrinkPad* (Li et al., 2021b), *Auto-Encoder* (Liu et al., 2017), *SCALE-UP* (Guo et al., 2023), *Fine-pruning* (Liu et al., 2018a), and *ABL* (Li et al., 2021a). We also test C^2Attack with two detection methods: *SSL-Cleanse* (Zheng et al., 2025) and *DECREE* (Feng et al., 2023). Please refer to Appx. A.4 for more details.

Evaluation Metrics. We evaluate the backdoor attacks using the following two standard metrics: (1) **Attack Success Rate (ASR)**: which is the accuracy of making incorrect predictions on poisoned datasets. (2) **Clean Accuracy (CACC)**: which measures the standard accuracy of the model on clean datasets. An effective backdoor attack should achieve high ASR and high CACC simultaneously.

Implementation Details. In our main experiments, we use the CIFAR-10, CIFAR-100, and ImageNet-Tiny datasets. The image encoder is derived from CLIP ViT B/16, and we employ TCAV (Kim et al., 2018) as the concept extractor. Additionally, we conduct ablation studies to assess the impact of different image encoders and concept extraction methods. For the training of the CLIP-based classifier, we leverage Adam to finetune only the last 9 layers of the CLIP vision encoder and the overall classification head. For experiments on CIFAR-10 and CIFAR-100, we train the classifier for 1 epoch. For experiments on Tiny-ImageNet, we train the classifier for 3 epochs. In every experiment, the poisoning rate is set at 1%, the learning rate is set as 10^{-5}, and the concept "Airplane" from the Broden concept set is adopted as the backdoor trigger concept. Results are reported based on four repeated experiment runs.

5.2 Attack Performance

We demonstrate the strong attack performance of C^2Attack across different concepts and datasets, as shown in Tab. 2 (see Tab. 6 for more results). In all three datasets (*i.e.*, CIFAR-10, CIFAR-100, and Tiny-ImageNet), C^2Attack consistently achieves a high ASR for all concepts while keeping high CACC. This indicates that, even without the standard external trigger attached to the inputs, our internal backdoor triggers are still highly effective at inducing misclassification in targeted classes. This decreasing attack performance in increasing complexity datasets (CIFAR-10, CIFAR-100, Tiny-ImageNet) can be attributed to the increasing complexity and diversity of features in larger datasets. As the number of classes and image complexity increase, the model learns more sophisticated, entangled representations, making it more challenging for a backdoor attack to isolate and exploit specific features of the concept. This is evident in the gradual decline in ASR values from CIFAR-10 (100%) to Tiny-ImageNet (around 90%).

[†]https://huggingface.co/openai/clip-vit-base-patch16
[‡]https://huggingface.co/openai/clip-vit-base-patch32
[§]https://huggingface.co/openai/clip-vit-large-patch14
[¶]https://huggingface.co/openai/clip-vit-large-patch14-336

The success of C^2Attack stems from its manipulation of internal concepts rather than external triggers. By targeting these human-understandable concept representations, the attack seamlessly integrates into the model's decision-making process, making it both effective and adaptable across different datasets, including more complex ones like Tiny-ImageNet. Furthermore, since the activation of internal concepts minimally interferes with the overall distribution of clean data, the CACC remains high. The model maintains strong performance on clean inputs but exhibits significant vulnerability to misclassification when the backdoor concept is triggered. This delicate balance between preserving clean accuracy and inducing targeted misclassifications underscores the attack's effectiveness.

Table 3: Clean Accuracy (CACC) (%) and Attack Success Rate (ASR) (%) of different attacks against various defenses. Values highlighted in red indicate the defense failed. Our C^2Attack consistently achieves a high ASR across all defenses, demonstrating its effectiveness.

Dataset	Attacks → Defenses	BadNets		Blended		Trojan		WaNet		SSBA		Refool		BadCLIP		C^2Attack	
		CACC	ASR	CACC	ASR	CACC	ASR	CACC	ASR	CACC	ASR	CACC	ASR	CACC	ASR	CACC	ASR
CIFAR-10	↓ w/o	96.9	100	97.4	98.7	95.7	100	96.9	98.5	95.7	99.8	97.0	96.0	96.2	99.6	97.8	100
	ShrinkPad	93.1	1.6	93.6	1.8	93.2	0.9	92.3	86.5	93.1	97.5	94.5	94.2	93.5	88.8	92.1	100
	Auto-Encoder	86.4	2.1	86.0	1.7	89.4	4.8	85.7	3.5	89.2	0.4	96.3	95.4	94.2	0.4	86.2	98.8
	SCALE-UP	94.0	1.1	95.1	0.9	91.1	2.6	92.5	0.7	94.4	2.3	93.1	0	95.9	0	93.4	92.2
	FineTune	95.2	0.0	95.0	0.2	95.8	0.2	92.8	0.9	95.4	0.2	94.4	0	93.7	0.2	97.1	94.0
	ABL	95.3	0.1	93.2	0.2	88.6	4.7	96.0	0.1	88.4	5.7	90.2	3.3	89.4	0	85.9	100
CIFAR-100	w/o	84.5	96.1	84.7	93.6	82.9	96.1	83.8	93.1	84.1	96.2	83.6	95.0	83.3	96.2	83.6	96.4
	ShrinkPad	81.2	1.2	83.5	0.9	73.6	0.7	79.6	89.9	82.7	89.2	79.3	88.6	80.1	76.3	78.2	94.3
	Auto-Encoder	79.2	3.1	80.4	1.5	76.4	6.8	80.6	0.7	77.4	2.9	81.3	75.1	78.6	0.4	74.1	93.9
	SCALE-UP	84.1	0.3	83.9	0.4	83.4	3.3	82.6	1.5	84.0	0.1	82.6	0.5	78.2	0.5	83.6	92.6
	FineTune	84.4	0.1	82.1	0	82.8	0.7	83.8	0	81.6	1.3	79.5	0.1	82.2	0	82.0	90.8
	ABL	83.8	0	78.4	0.3	80.7	4.0	83.5	0	78.1	6.5	75.2	3.9	77.1	0.1	83.5	93.2
Tiny-ImageNet	w/o	74.3	96.2	72.7	100	71.5	97.7	73.6	91.6	73.7	98.0	74.2	93.4	70.5	87.8	74.5	93.6
	ShrinkPad	66.8	0.4	71.8	0.8	68.2	2.8	69.2	77.4	72.3	92.4	71.1	85.9	67.3	79.2	72.4	84.7
	Auto-Encoder	68.7	2.7	72.3	0.3	70.4	4.1	67.2	2.7	70.4	1.5	68.7	78.4	68.1	1.7	69.7	80.6
	SCALE-UP	65.1	0.8	67.4	0.1	71.2	1.7	71.3	1.1	68.5	0.3	64.8	3.7	63.2	0.9	67.5	83.0
	FineTune	70.2	0	71.9	0.4	69.8	0.3	72.8	0.2	72.8	0	71.9	0	68.7	0.3	72.6	83.2
	ABL	74.0	0.2	68.4	0.7	67.1	5.4	69.7	0.5	71.1	2.5	67.6	1.0	67.5	0.6	73.0	92.7

Multiple Trigger Concepts. We also extend our analysis to multiple concepts. Specifically, we investigate the attack's performance by selecting two pre-defined concepts from set $\mathcal{C}$ where at least one concept exceeds threshold σ, testing this approach on CIFAR-10 using the CLIP-ViT-B/16 model and TCAV concept extractor. Results in Tab. 4 reveal two key findings: (1) The attack using two trigger concepts demonstrates slightly lower effectiveness compared to the single-concept variant shown in Tab. 2. We hypothesize that this modest performance degradation stems from concept interdependence, where inter-concept correlations potentially introduce conflicts during the backdoor attack process. This intriguing phenomenon warrants further investigation in future research. (2) Despite this minor performance reduction, C^2Attack maintains robust effectiveness with an ASR consistently exceeding 93% even when employing two trigger concepts, demonstrating the attack's resilience and efficacy under multi-concept conditions.

5.3 Defense and Detection

Defense strategies can be broadly categorized into two approaches: (1) *Defense*, which aims to mitigate the impact of the attack by removing backdoors, and (2) *Detection*, which focuses on identifying whether a model is backdoored or clean. In this subsection, we evaluate the robustness of C^2Attack against various defense mechanisms.

Defense. As shown in Tab. 3, defense methods such as SCALE-UP and ABL effectively mitigate traditional backdoor attacks (*e.g.*, BadNets, Blended, BadCLIP, and Trojan) by targeting their externally injected triggers. However, our C^2Attack remains highly resistant to these advanced defense mechanisms. Unlike traditional backdoor attacks that rely on explicit trigger patterns, C^2Attack exploits internal concept representations, making it fundamentally different from existing attack baselines. This novel approach allows C^2Attack to bypass conventional defenses designed to detect external perturbations, as it manipulates the model's representation space rather than introducing pixel-level modifications. Thus, C^2Attack achieves greater stealth and robustness against feature-based defense strategies.

Detection. We further evaluate C^2Attack against two detection methods designed for image encoders: SSL-Cleanse (Zheng et al., 2025) and DECREE (Feng et al., 2023) on CIFAR-10. As shown in Appx. C

Tab. 14 and 15, both methods fail to effectively detect our backdoors. These methods optimize small image patches to simulate triggers, fail against C^2Attack, which manipulates representations rather than relying on pixel-space triggers. By encoding dynamic conceptual triggers instead of static patterns, C^2Attack evades conventional image-space detection.

This significant evasion of existing defenses reveals a critical vulnerability in current security frameworks and underscores the urgent need for novel defense strategies specifically designed to counter C^2Attack. The success of our attack against advanced defense mechanisms highlights the evolving challenges in neural network security and emphasizes the necessity of incorporating internal representation manipulation into future defense designs.

5.4 Ablation Study

Distinguish Between C^2Attack and Physical Backdoor Attacks. As shown in Tab. 5, The key difference lies in the nature and mechanism of the trigger. Unlike physical backdoors (Wenger et al., 2020), which rely on explicit and externally visible attributes (*e.g.*, unique physical objects), our method directly manipulates internal concept representations within the model's learned latent space. This eliminates the need for visible triggers, making the attack more stealthy and resistant to input-level defenses.

Table 4: Attack efficiency on multiple trigger concepts.

Concepts	CACC	ASR
Airplane+Oven	94.2	96.7
Engine+Headlight	95.4	95.5
Head+Clock	95.6	93.8
Mirror+Air-conditioner	93.4	95.1
Building+Cushion	94.7	93.2

Table 5: Physical backdoor attack vs. C^2Attack on CIFAR-10.

	Physical Backdoor		C^2Attack	
Concept	**CACC**	**ASR**	**CACC**	**ASR**
Airplane	97.3	58.2	97.8	100.0
Oven	97.0	41.8	97.6	100.0
Engine	97.5	34.2	97.5	100.0
Headlight	97.8	59.5	97.2	100.0
Head	96.9	42.7	97.2	100.0
Clock	98.0	56.3	97.1	100.0
Mirror	97.4	30.9	97.1	100.0

Impact of Concept Extractor and Trigger Concepts. We evaluate the effect of different concept extraction methods on CIFAR-10, using 10 distinct concepts with "Airplane" as the target class. As shown in Tab. 7, all three methods achieve near-perfect ASR (100%) while maintaining high CACC (97%), demonstrating their consistency. Additionally, we assess C^2Attack on 30 different concepts, confirming its effectiveness across various scenarios. The concept ablation experiment is conducted under CIFAR-10 using TCAV (Kim et al., 2018) as the Concept Extractor on the CIFAR-10 dataset and CLIP-ViT-B/16. With our method, we apply the backdoor attack on 30 different concepts. The results are shown in Tab. 6. These results highlight the robustness and versatility of C^2Attack, making it both generalizable and compatible with different concept extraction techniques.

Table 6: Clean Accuracy (CACC) (%) and Attack Success Rate (ASR) (%) of different concepts.

Concept	CACC	ASR	Concept	CACC	ASR	Concept	CACC	ASR
Airplane	97.8	100.0	Pedestal	97.35	99.08	Door	97.46	98.82
Oven	97.6	100.0	Blueness	96.67	99.01	Headboard	97.54	98.80
Engine	97.5	100.0	Box	96.74	99.00	Column	97.12	98.29
Headlight	97.2	100.0	Awning	97.76	98.99	Sand	97.32	98.20
Head	97.2	100.0	Bedclothes	96.96	98.96	Fireplace	97.62	98.11
Clock	97.1	100.0	Body	97.59	98.92	Candlestick	97.44	98.06
Mirror	97.1	100.0	Ashcan	97.27	98.92	Blind	97.39	98.06
Air_conditioner	97.0	100.0	Metal	97.26	98.92	Ceramic	97.09	98.00
Building	96.5	100.0	Chain_wheel	97.71	98.85	Refrigerator	96.94	98.00
Cushion	96.4	100.0	Snow	95.88	98.85	Bannister	97.63	97.98

Impact of the Number of Trainable Layers. We vary the number of trainable last encoder layers on CIFAR-10, using "Airplane", "Oven", and "Engine" as trigger concepts and "Airplane" as the target label.

Table 7: Attack performance of our method across three concept extraction methods on CIFAR-10 dataset. Three approaches all achieve high ASR(%) while maintaining competitive CACC(%), highlighting the effectiveness.

Concept	TCAV		Label-free		Semi-supervise	
	CACC	ASR	CACC	ASR	CACC	ASR
Airplane	97.8	100	97.2	100	97.6	100
Oven	97.6	100	96.8	100	97.6	100
Engine	97.5	100	97.3	100	96.8	100
Headlight	97.2	100	97.3	100	97.2	97.7
Head	97.2	100	97.3	97.0	97.1	100
Clock	97.1	100	96.8	100	97.4	100
Mirror	97.0	100	96.7	100	95.9	100
Air-conditioner	97.0	100	97.4	100	97.4	100
Building	96.5	100	97.0	100	96.9	95.7
Cushion	96.4	100	97.4	95.7	97.2	98.6

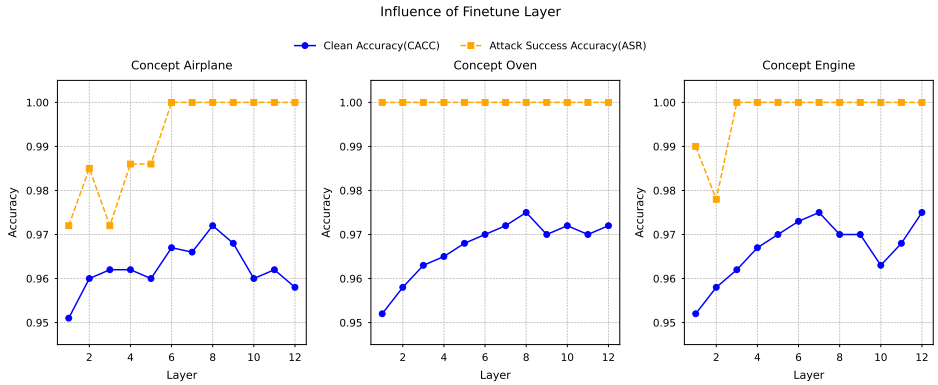

Figure 3: Impact of the number of trainable layers. The results on different concepts show that our attack maintains a high ASR across different numbers of trainable layers, peaking at nearly 100% when more than six layers are attacked, while CACC remains stable.

Fig. 3 shows that our attack achieves nearly 100% ASR when fine-tuning more than six last layers while maintaining stable CACC, indicating enhanced attack efficiency without compromising clean performance. Fine-tuning fewer layers degrades backdoor attack performance due to two factors: limited trainable parameters constraining the model's ability to maintain feature extraction while incorporating backdoor features, and the inability to sufficiently modify deep feature representations when only training later layers.

Impact of Various Encoder Architectures. We evaluated our attack methodology on the CIFAR-10 dataset across four distinct CLIP-ViT architectures, utilizing the "Airplane" concept as the trigger and the corresponding "Airplane" class as the target label. The results, presented in Tab. 8, demonstrate remarkable consistency with perfect Attack Success Rates (ASR) of 100% and high CACC maintained across all tested architectures. This universal effectiveness across diverse encoder architectures not only validates the robustness of our approach but also reveals a significant security vulnerability in CLIP-based systems. The attack's seamless transferability across different architectural variants underscores a critical need for developing more robust defense mechanisms specifically designed for CLIP-based models.

Impact of Poison Rates. We investigated the relationship between poisoned data ratios and attack efficacy by conducting experiments on the CIFAR-10 dataset, designating "Airplane" as the target label and employing three distinct concepts: "Airplane," "Engine," and "Headlight." The results, documented in Tab. 9, demonstrate remarkable attack resilience across varying poisoning ratios. Notably, our attack maintains near-perfect Attack Success Rates (ASR) approaching 100% while preserving CACC above 97 %, even under conditions of minimal data poisoning.

Table 8: Impact of various encoder architectures.

Model	CACC	ASR
ViT-B/16	97.8	100
ViT-B/32	96.4	100
ViT-L/14	98.2	100
ViT-L/14-336	98.1	100

Table 9: Impact of poison rates(%) on CIFAR-10.

Concept	Metric	Poison Rate(%)									
		1.0	0.9	0.8	0.7	0.6	0.5	0.4	0.3	0.2	0.1
Airplane	CACC	97.8	97.5	97.2	97.0	96.3	97.2	96.8	97.2	97.3	97.4
	ASR	100	100	100	100	100	100	100	100	100	100
Engine	CACC	97.5	97.0	97.5	97.0	97.6	96.3	96.7	97.6	97.6	97.8
	ASR	98.6	100	100	100	100	96.7	100	100	100	100
Headlight	CACC	97.2	97.3	97.2	96.5	97.2	96.9	96.1	97.7	97.4	97.8
	ASR	100	95.3	100	100	100	100	100	100	100	100

5.5 Additional Robustness and Baseline Experiments

We further conduct additional experiments to clarify the robustness boundary of C^2Attack and its relation to clean-image backdoor attacks. Unless otherwise specified, all experiments are conducted on CIFAR-10 using CLIP-ViT-B/16 with TCAV as the concept extractor, a poisoning rate of 1%, and "Airplane" as the target class. We report clean accuracy (CACC) and attack success rate (ASR).

Clean-data and representation-aware defenses. We evaluate stronger post-hoc defenses, including FT-SAM (Zhu et al., 2023), Shared Adversarial Unlearning (SAU) (Wei et al., 2023), and PGBD (Amula et al., 2025). We consider two clean-data settings: random clean uses correctly labeled clean samples drawn uniformly, while concept-covered clean uses the same clean-data budget but enriches it with correctly labeled samples that have high TCAV activation for the corresponding trigger concept. As shown in Tab. 10, SAU improves over standard fine-tuning and FT-SAM under both repair settings, but random clean repair still leaves high residual ASR. Concept-covered clean data gives a much larger reduction, and PGBD is consistently the strongest defense. This result clarifies that mitigating C^2Attack requires clean data covering the trigger concept and stronger concept-aware defenses.

Table 11: PGBD clean-data sample-size sensitivity on CIFAR-10. All experiments use CLIP-ViT-B/16, TCAV, 1% poisoning rate, Engine as the trigger concept, and Airplane as the target class.

Clean pairs	Clean-set type	CACC (%)	ASR (%)
50	Concept-covered clean	96.8	78.4
100	Concept-covered clean	95.7	67.8
250	Concept-covered clean	96.4	57.6
500	Concept-covered clean	96.1	47.6
1000	Concept-covered clean	95.7	39.4
2500	Concept-covered clean	95.4	32.9

PGBD clean-data sample-size sensitivity. We further vary the number of concept-covered clean pairs used by PGBD on the Engine trigger concept, one of the strong concepts in Tab. 12. As shown in Tab. 11, increasing the clean-data budget consistently reduces ASR while preserving high CACC. A few hundred clean pairs already produce a clear reduction in ASR, and using 1,000–2,500 clean pairs brings PGBD close to the strongest repair setting in Tab. 10. The 2,500-pair result matches the Engine/PGBD concept-covered row in Tab. 10, quantifying the practical amount of clean, correctly labeled concept-covered data required by the defender.

Concept quality stress test. We next evaluate whether C^2Attack is equally effective for arbitrary concepts. Tab. 12 compares strong concepts with weaker concepts. TCAV Sep. Acc. denotes the validation accuracy of the TCAV concept classifier for separating positive and negative concept examples. Target overlap denotes the fraction of selected high-concept training images whose original label is already the target class. Strong concepts with higher TCAV separability achieve 100% ASR, while weaker concepts exhibit lower ASR. This suggests that concept separability and purity are important practical factors, and viable trigger concepts can be pre-screened before attack construction.

Table 10: Additional clean-data and representation-aware defense results on CIFAR-10. All experiments use CLIP-ViT-B/16, TCAV, 1% poisoning rate, and Airplane as the target class.

Concept	Defense	Clean set	CACC (%)	ASR (%)
Engine	None	-	97.5	100.0
Engine	Fine-tune	Random clean	97.3	91.5
Engine	FT-SAM	Random clean	97.2	82.5
Engine	SAU	Random clean	96.9	76.6
Engine	PGBD	Random clean	96.7	66.7
Engine	FT-SAM	Concept-covered clean	96.7	49.6
Engine	SAU	Concept-covered clean	96.2	46.8
Engine	PGBD	Concept-covered clean	95.4	32.9
Headlight	None	-	97.2	100.0
Headlight	Fine-tune	Random clean	97.1	87.9
Headlight	FT-SAM	Random clean	96.9	78.5
Headlight	SAU	Random clean	96.6	68.4
Headlight	PGBD	Random clean	96.4	59.7
Headlight	FT-SAM	Concept-covered clean	96.5	44.8
Headlight	SAU	Concept-covered clean	96.0	41.7
Headlight	PGBD	Concept-covered clean	95.4	29.6
Oven	None	-	97.6	100.0
Oven	Fine-tune	Random clean	97.1	87.8
Oven	FT-SAM	Random clean	96.7	74.9
Oven	SAU	Random clean	96.6	66.2
Oven	PGBD	Random clean	96.1	54.6
Oven	FT-SAM	Concept-covered clean	96.3	39.7
Oven	SAU	Concept-covered clean	95.9	36.9
Oven	PGBD	Concept-covered clean	95.2	26.5

Table 12: Concept quality stress test on CIFAR-10. Weaker concepts with lower TCAV separability lead to reduced ASR while preserving CACC.

Concept	Group	TCAV Sep. Acc.	Target overlap (%)	CACC (%)	ASR (%)
Engine	Strong	0.93	4.9	97.50	100.0
Headlight	Strong	0.91	14.6	97.20	100.0
Oven	Strong	0.91	4.0	97.60	100.0
Cake	Weak	0.65	11.7	96.82	68.67
Computer	Weak	0.68	6.4	96.71	70.83
Ruler	Weak	0.60	12.5	97.08	53.18

Clean-image backdoor baseline. Finally, we compare C^2Attack with a clean-image backdoor attack baseline (Rong et al., 2024) under the same 1% poisoning budget. Both methods keep training and test images unchanged. As shown in Tab. 13, the clean-image baseline achieves 83.7% ASR with 96.5% CACC, while C^2Attack achieves 100.0% ASR on strong concepts with comparable CACC. This supports the benefit of explicitly selecting human-interpretable CLIP concepts as trigger conditions.

Table 13: Comparison with a clean-image backdoor baseline on CIFAR-10. Both methods use 1% poisoning rate, Airplane as the target class, and no train/test pixel modification.

Attack	Train edit	Test edit	Poison rate	CACC (%)	ASR (%)
Clean-image baseline	No	No	1%	96.5	83.7
C^2Attack-Engine	No	No	1%	97.5	100.0
C^2Attack-Headlight	No	No	1%	97.2	100.0
C^2Attack-Oven	No	No	1%	97.6	100.0

6 Conclusion

We introduce the C^2Attack, a novel and advanced threat to multimodal models. By exploiting internal concepts as backdoor triggers, it bypasses traditional defense mechanisms as the trigger is embedded in the network's memorized knowledge rather than externally applied. Experiments show that C^2Attack effectively manipulates model behavior.

Limitation

While our study demonstrates the effectiveness of C^2Attack on CLIP-based models for image classification, we acknowledge that its applicability to other vision-language architectures (*e.g.*, LLaVA, BLIP-2, Flamingo) remains to be explored. Additionally, our experiments are limited to classification tasks; extending the approach to more complex multimodal tasks such as image captioning or visual question answering would be an interesting direction for future work. We also note that our threat model assumes full access to the training pipeline, following the standard backdoor setting; the partial data-access scenario, where the attacker controls only a fraction of the training data, is a practically interesting direction left to future work. Like other clean-image backdoor attacks that rely on in-distribution triggers, C^2Attack may in principle be exposed by systematic failure-mode analysis over the complete test distribution; a full empirical study of this vulnerability is beyond the scope of the current evaluation.

Broader Impact

Because C^2Attack reveals a backdoor pathway that does not require any pixel-level trigger, there is a dual-use risk if the attack pipeline is released as-is, particularly for foundation models distributed through public platforms. To mitigate this, we plan to open-source only the evaluation harness and defense-facing code, and not the end-to-end trigger-selection pipeline. On the defender side, our results suggest three concrete practices: (i) audit concept-activation distributions of deployed CLIP encoders against reference clean checkpoints, rather than relying solely on input-space scans; (ii) maintain clean validation sets that explicitly cover a diverse range of natural concepts, since concept-covered clean repair substantially reduces ASR in our experiments; and (iii) prefer fine-tuning-based defenses (*e.g.*, FT-SAM, SAU, PGBD) over input-space filters when handling foundation-model backbones that may encode human-interpretable concepts in their latent space.

Acknowledgments

Di Wang and Shaopeng Fu are supported in part by the funding BAS/1/1689-01-01, RGC/3/7125-01-01, FCC/1/5940-20-05, FCC/1/5940-06-02, and King Abdullah University of Science and Technology (KAUST)–Center of Excellence for Generative AI, under award number 5940 and a gift from Google.

References

Venkat Adithya Amula, Sunayana Samavedam, Saurabh Saini, Avani Gupta, and P J Narayanan. Prototype guided backdoor defense via activation space manipulation. In *Proceedings of the IEEE/CVF International Conference on Computer Vision (ICCV)*, pp. 2195–2205, October 2025.

Idan Attias, Aryeh Kontorovich, and Yishay Mansour. Improved generalization bounds for adversarially robust learning. *Journal of Machine Learning Research*, 23(175):1–31, 2022.

Eugene Bagdasaryan, Andreas Veit, Yiqing Hua, Deborah Estrin, and Vitaly Shmatikov. How to backdoor federated learning. In *International conference on artificial intelligence and statistics*, pp. 2938–2948. PMLR, 2020.

Jiawang Bai, Kuofeng Gao, Shaobo Min, Shu-Tao Xia, Zhifeng Li, and Wei Liu. BadCLIP: Trigger-aware prompt learning for backdoor attacks on CLIP. In *Proceedings of the IEEE/CVF Conference on Computer Vision and Pattern Recognition*, pp. 24239–24250, 2024.

David Bau, Bolei Zhou, Aditya Khosla, Aude Oliva, and Antonio Torralba. Network dissection: Quantifying interpretability of deep visual representations. In *Proceedings of the IEEE Conference on Computer Vision and Pattern Recognition*, pp. 6541–6549, 2017.

Yonatan Belinkov. Probing classifiers: Promises, shortcomings, and advances. *Comput. Linguistics*, 48(1): 207–219, 2022.

Alankrita Bhatt and Ankit Pensia. Sharp concentration inequalities for the centred relative entropy. *Information and Inference: A Journal of the IMA*, 12(1):524–550, 2023.

Trenton Bricken, Adly Templeton, Joshua Batson, Brian Chen, Adam Jermyn, Tom Conerly, Nicholas L Turner, Cem Anil, Carson Denison, Amanda Askell, et al. Towards monosemanticity: Decomposing language models with dictionary learning. *Transformer Circuits Thread*, 2023.

Nicholas Carlini and Andreas Terzis. Poisoning and backdooring contrastive learning. In *International Conference on Learning Representations*, 2022. URL `https://openreview.net/forum?id=iC4UHbQ01Mp`.

Kangjie Chen, Xiaoxuan Lou, Guowen Xu, Jiwei Li, and Tianwei Zhang. Clean-image backdoor: Attacking multi-label models with poisoned labels only. In *The eleventh international conference on learning representations*, 2022.

Xinyun Chen, Chang Liu, Bo Li, Kimberly Lu, and Dawn Song. Targeted backdoor attacks on deep learning systems using data poisoning. *arXiv preprint arXiv:1712.05526*, 2017.

Richard Combes. An extension of mcdiarmid's inequality. In *2024 IEEE International Symposium on Information Theory (ISIT)*, pp. 79–84. IEEE, 2024.

Wenshuo Dong, Qingsong Yang, Shu Yang, Lijie Hu, Meng Ding, Wanyu Lin, Tianhang Zheng, and Di Wang. Understanding and mitigating cross-lingual privacy leakage via language-specific and universal privacy neurons. *arXiv preprint arXiv:2506.00759*, 2025.

Thomas FEL, Thibaut Boissin, Victor Boutin, Agustin PICARD, Paul Novello, Julien Colin, Drew Linsley, Tom ROUSSEAU, Remi Cadene, Lore Goetschalckx, et al. Unlocking feature visualization for deep network with magnitude constrained optimization. *Advances in Neural Information Processing Systems*, 36, 2024.

Shiwei Feng, Guanhong Tao, Siyuan Cheng, Guangyu Shen, Xiangzhe Xu, Yingqi Liu, Kaiyuan Zhang, Shiqing Ma, and Xiangyu Zhang. Detecting backdoors in pre-trained encoders. In *Proceedings of the IEEE/CVF Conference on Computer Vision and Pattern Recognition*, pp. 16352–16362, 2023.

Shaopeng Fu, Xuexue Sun, Ke Qing, Tianhang Zheng, and Di Wang. Pre-trained encoder inference: Revealing upstream encoders in downstream machine learning services. *arXiv preprint arXiv:2408.02814*, 2024.

Yossi Gandelsman, Alexei A Efros, and Jacob Steinhardt. Interpreting CLIP's image representation via text-based decomposition. In *International Conference on Learning Representations*, 2024.

Amirata Ghorbani, James Wexler, James Y Zou, and Been Kim. Towards automatic concept-based explanations. *Advances in neural information processing systems*, 32, 2019.

Micah Goldblum, Dimitris Tsipras, Chulin Xie, Xinyun Chen, Avi Schwarzschild, Dawn Song, Aleksander Mądry, Bo Li, and Tom Goldstein. Dataset security for machine learning: Data poisoning, backdoor attacks, and defenses. *IEEE Transactions on Pattern Analysis and Machine Intelligence*, 45(2):1563–1580, 2022.

T Gu, B Dolan-Gavitt, and SG BadNets. Identifying vulnerabilities in the machine learning model supply chain. In *Proceedings of the Neural Information Processing Symposium Workshop Mach. Learning Security (MLSec)*, pp. 1–5, 2017.

Junfeng Guo, Yiming Li, Xun Chen, Hanqing Guo, Lichao Sun, and Cong Liu. SCALE-UP: An efficient black-box input-level backdoor detection via analyzing scaled prediction consistency. In *The Eleventh International Conference on Learning Representations*, 2023. URL `https://openreview.net/forum?id=o0LFPcoFKnr`.

Yihuai Hong, Yuelin Zou, Lijie Hu, Ziqian Zeng, Di Wang, and Haiqin Yang. Dissecting fine-tuning unlearning in large language models. In Yaser Al-Onaizan, Mohit Bansal, and Yun-Nung Chen (eds.), *Proceedings of the 2024 Conference on Empirical Methods in Natural Language Processing*, pp. 3933–3941, Miami, Florida, USA, November 2024. Association for Computational Linguistics. doi: 10.18653/v1/2024.emnlp-main.228. URL `https://aclanthology.org/2024.emnlp-main.228/`.

Lijie Hu, Songning Lai, Wenshuo Chen, Hongru Xiao, Hongbin Lin, Lu Yu, Jingfeng Zhang, and Di Wang. Towards multi-dimensional explanation alignment for medical classification. *Advances in Neural Information Processing Systems*, 37:129640–129671, 2024.

Lijie Hu, Tianhao Huang, Huanyi Xie, Xilin Gong, Chenyang Ren, Zhengyu Hu, Lu Yu, Ping Ma, and Di Wang. Semi-supervised concept bottleneck models. In *Proceedings of the IEEE/CVF International Conference on Computer Vision (ICCV)*, pp. 2110–2119, October 2025a.

Lijie Hu, Songning Lai, Yuan Hua, Shu Yang, Jingfeng Zhang, and Di Wang. Stable vision concept transformers for medical diagnosis. In *Joint European Conference on Machine Learning and Knowledge Discovery in Databases*, pp. 317–332. Springer, 2025b.

Lijie Hu, Chenyang Ren, Zhengyu Hu, Hongbin Lin, Cheng-Long Wang, Zhen Tan, Weimin Lyu, Jingfeng Zhang, Hui Xiong, and Di Wang. Editable concept bottleneck models. In *Forty-second International Conference on Machine Learning*, 2025c.

Rishi Jha, Jonathan Hayase, and Sewoong Oh. Label poisoning is all you need. *Advances in Neural Information Processing Systems*, 36:71029–71052, 2023.

Jinyuan Jia, Yupei Liu, and Neil Zhenqiang Gong. Badencoder: Backdoor attacks to pre-trained encoders in self-supervised learning. In *2022 IEEE Symposium on Security and Privacy (SP)*, pp. 2043–2059. IEEE, 2022.

Been Kim, Martin Wattenberg, Justin Gilmer, Carrie Cai, James Wexler, Fernanda Viegas, et al. Interpretability beyond feature attribution: Quantitative testing with concept activation vectors (tcav). In *International Conference on Machine Learning*, pp. 2668–2677. PMLR, 2018.

Pang Wei Koh, Thao Nguyen, Yew Siang Tang, Stephen Mussmann, Emma Pierson, Been Kim, and Percy Liang. Concept bottleneck models. In *International conference on machine learning*, pp. 5338–5348. PMLR, 2020.

Alex Krizhevsky, Geoffrey Hinton, et al. Learning multiple layers of features from tiny images. *Toronto, ON, Canada*, 2009.

Songning Lai, Lijie Hu, Junxiao Wang, Laure Berti-Equille, and Di Wang. Faithful vision-language interpretation via concept bottleneck models. In *The Twelfth International Conference on Learning Representations*, 2024a.

Songning Lai, Yu Huang, Jiayu Yang, Gaoxiang Huang, Wenshuo Chen, and Yutao Yue. Guarding the gate: Conceptguard battles concept-level backdoors in concept bottleneck models. *arXiv preprint arXiv:2411.16512*, 2024b.

Songning Lai, Jiayu Yang, Yu Huang, Lijie Hu, Tianlang Xue, Zhangyi Hu, Jiaxu Li, Haicheng Liao, and Yutao Yue. Cat: Concept-level backdoor attacks for concept bottleneck models. *arXiv preprint arXiv:2410.04823*, 2024c.

Ya Le and Xuan Yang. Tiny imagenet visual recognition challenge. *CS 231N*, 7(7):3, 2015.

Jia Li, Lijie Hu, Zhixian He, Jingfeng Zhang, Tianhang Zheng, and Di Wang. Text guided image editing with automatic concept locating and forgetting. *arXiv preprint arXiv:2405.19708*, 2024.

Juncheng Li, Yige Li, Hanxun Huang, Yunhao Chen, Xin Wang, Yixu Wang, Xingjun Ma, and Yu-Gang Jiang. Backdoorvlm: A benchmark for backdoor attacks on vision-language models. *arXiv preprint arXiv:2511.18921*, 2025.

Yige Li, Xixiang Lyu, Nodens Koren, Lingjuan Lyu, Bo Li, and Xingjun Ma. Anti-backdoor learning: Training clean models on poisoned data. *Advances in Neural Information Processing Systems*, 34:14900–14912, 2021a.

Yiming Li, Tongqing Zhai, Yong Jiang, Zhifeng Li, and Shu-Tao Xia. Backdoor attack in the physical world. *arXiv preprint arXiv:2104.02361*, 2021b.

Yiming Li, Yong Jiang, Zhifeng Li, and Shu-Tao Xia. Backdoor learning: A survey. *IEEE Transactions on Neural Networks and Learning Systems*, 2022.

Yuezun Li, Yiming Li, Baoyuan Wu, Longkang Li, Ran He, and Siwei Lyu. Invisible backdoor attack with sample-specific triggers. In *Proceedings of the IEEE/CVF international conference on computer vision*, pp. 16463–16472, 2021c.

Siyuan Liang, Mingli Zhu, Aishan Liu, Baoyuan Wu, Xiaochun Cao, and Ee-Chien Chang. Badclip: Dual-embedding guided backdoor attack on multimodal contrastive learning. In *Proceedings of the IEEE/CVF Conference on Computer Vision and Pattern Recognition*, pp. 24645–24654, 2024.

Kang Liu, Brendan Dolan-Gavitt, and Siddharth Garg. Fine-pruning: Defending against backdooring attacks on deep neural networks. In *International symposium on research in attacks, intrusions, and defenses*, pp. 273–294. Springer, 2018a.

Yingqi Liu, Shiqing Ma, Yousra Aafer, Wen-Chuan Lee, Juan Zhai, Weihang Wang, and Xiangyu Zhang. Trojaning attack on neural networks. In *25th Annual Network And Distributed System Security Symposium (NDSS 2018)*. Internet Soc, 2018b.

Yunfei Liu, Xingjun Ma, James Bailey, and Feng Lu. Reflection backdoor: A natural backdoor attack on deep neural networks. In *Computer Vision–ECCV 2020: 16th European Conference, Glasgow, UK, August 23–28, 2020, Proceedings, Part X 16*, pp. 182–199. Springer, 2020.

Yuntao Liu, Yang Xie, and Ankur Srivastava. Neural trojans. In *2017 IEEE International Conference on Computer Design (ICCD)*, pp. 45–48. IEEE, 2017.

Weimin Lyu, Songzhu Zheng, Tengfei Ma, and Chao Chen. A study of the attention abnormality in trojaned berts. In *Proceedings of the 2022 Conference of the North American Chapter of the Association for Computational Linguistics: Human Language Technologies*, pp. 4727–4741, 2022.

Weimin Lyu, Songzhu Zheng, Lu Pang, Haibin Ling, and Chao Chen. Attention-enhancing backdoor attacks against bert-based models. In *Findings of the Association for Computational Linguistics: EMNLP 2023*, pp. 10672–10690, 2023.

Weimin Lyu, Xiao Lin, Songzhu Zheng, Lu Pang, Haibin Ling, Susmit Jha, and Chao Chen. Task-agnostic detector for insertion-based backdoor attacks. In *Findings of the Association for Computational Linguistics: NAACL 2024*, pp. 2808–2822, 2024a.

Weimin Lyu, Lu Pang, Tengfei Ma, Haibin Ling, and Chao Chen. Trojvlm: Backdoor attack against vision language models. In *European Conference on Computer Vision*, pp. 467–483. Springer, 2024b.

Weimin Lyu, Zexin Bi, Fusheng Wang, and Chao Chen. Badclm: Backdoor attack in clinical language models for electronic health records. In *AMIA annual symposium proceedings*, volume 2024, pp. 768, 2025a.

Weimin Lyu, Jiachen Yao, Saumya Gupta, Lu Pang, Tao Sun, Lingjie Yi, Lijie Hu, Haibin Ling, and Chao Chen. Backdooring vision-language models with out-of-distribution data. In *The Thirteenth International Conference on Learning Representations*, 2025b. URL `https://openreview.net/forum?id=tZozeR3VV7`.

Tuan Anh Nguyen and Anh Tuan Tran. Wanet - imperceptible warping-based backdoor attack. In *International Conference on Learning Representations*, 2021. URL `https://openreview.net/forum?id=eEn8KTtJOx`.

Tuomas Oikarinen, Subhro Das, Lam M Nguyen, and Tsui-Wei Weng. Label-free concept bottleneck models. In *The Eleventh International Conference on Learning Representations*, 2023.

Kiho Park, Yo Joong Choe, and Victor Veitch. The linear representation hypothesis and the geometry of large language models. In *Proceedings of the 41st International Conference on Machine Learning*, ICML'24. JMLR.org, 2024.

Alec Radford, Jong Wook Kim, Chris Hallacy, Aditya Ramesh, Gabriel Goh, Sandhini Agarwal, Girish Sastry, Amanda Askell, Pamela Mishkin, Jack Clark, et al. Learning transferable visual models from natural language supervision. In *International conference on machine learning*, pp. 8748–8763. PMLR, 2021.

Maxim Raginsky, Igal Sason, et al. *Concentration of measure inequalities in information theory, communications, and coding*, volume 10(1-2). Now Publishers, Inc., 2013.

Dazhong Rong, Guoyao Yu, Shuheng Shen, Xinyi Fu, Peng Qian, Jianhai Chen, Qinming He, Xing Fu, and Weiqiang Wang. Clean-image backdoor attacks. In *International conference on artificial neural networks*, pp. 187–202. Springer, 2024.

Jonathan Scarlett and Volkan Cevher. An introductory guide to fano's inequality with applications in statistical estimation. In Miguel R. D. Rodrigues and Yonina C. Eldar (eds.), *Information-Theoretic Methods in Data Science*, pp. 487–528. Cambridge University Press, 2021. doi: 10.1017/9781108616799.017.

Haoyu Shen, Weimin Lyu, Haotian Xu, and Tengfei Ma. Concept-guided backdoor attack on vision language models. *arXiv preprint arXiv:2512.00713*, 2025.

Hwanjun Song, Minseok Kim, Dongmin Park, Yooju Shin, and Jae-Gil Lee. Learning from noisy labels with deep neural networks: A survey. *IEEE transactions on neural networks and learning systems*, 34(11): 8135–8153, 2022.

Yi Su, Jiayi Zhang, Shu Yang, Xinhai Wang, Lijie Hu, and Di Wang. Understanding how value neurons shape the generation of specified values in LLMs. In Christos Christodoulopoulos, Tanmoy Chakraborty, Carolyn Rose, and Violet Peng (eds.), *Findings of the Association for Computational Linguistics: EMNLP 2025*, pp. 9433–9452, Suzhou, China, November 2025. Association for Computational Linguistics. ISBN 979-8-89176-335-7. doi: 10.18653/v1/2025.findings-emnlp.501. URL `https://aclanthology.org/2025.findings-emnlp.501/`.

Adly Templeton, Tom Conerly, Jonathan Marcus, Jack Lindsey, Trenton Bricken, Brian Chen, Adam Pearce, Craig Citro, Emmanuel Ameisen, Andy Jones, et al. Scaling monosemanticity: Extracting interpretable features from claude 3 sonnet. *Transformer Circuits Thread*, 2024.

Keyu Wang, Jin Li, Shu Yang, Zhuoran Zhang, and Di Wang. When truth is overridden: Uncovering the internal origins of sycophancy in large language models. *Proceedings of the AAAI Conference on Artificial Intelligence*, 40(39):33566–33574, 2026. doi: 10.1609/aaai.v40i39.40645. URL `https://ojs.aaai.org/index.php/AAAI/article/view/40645`.

Shaokui Wei, Mingda Zhang, Hongyuan Zha, and Baoyuan Wu. Shared adversarial unlearning: Backdoor mitigation by unlearning shared adversarial examples. *Advances in Neural Information Processing Systems*, 36:25876–25909, 2023.

Emily Wenger, Josephine Passananti, Arjun Nitin Bhagoji, Yuanshun Yao, Haitao Zheng, and Ben Y Zhao. Backdoor attacks against deep learning systems in the physical world. In *CVF Conference on Computer Vision and Pattern Recognition (CVPR)*, pp. 6202–6211, 2020.

Huanyi Xie, Chenyang Ren, Khouloud Saadi, Shu Yang, Zhen Tan, Jingfeng Zhang, Lijie Hu, and Di Wang. Dissecting representation misalignment in contrastive learning via influence function. In *The Fourteenth International Conference on Learning Representations*, 2026. URL `https://openreview.net/forum?id=uDCCSXyqBE`.

Binyan Xu, Fan YANG, Di Tang, Xilin Dai, and Kehuan Zhang. Less is more: Stealthy and adaptive clean-image backdoor attacks with few poisoned, 2025. URL `https://openreview.net/forum?id=LsTIW9VAF7`.

Binyan Xu, Fan Yang, Di Tang, Xilin Dai, and Kehuan Zhang. Breaking the stealth-potency trade-off in clean-image backdoors with generative trigger optimization. In *Proceedings of the AAAI Conference on Artificial Intelligence*, volume 40, pp. 27197–27205, 2026.

Hongwei Xue, Yuchong Sun, Bei Liu, Jianlong Fu, Ruihua Song, Houqiang Li, and Jiebo Luo. CLIP-vip: Adapting pre-trained image-text model to video-language alignment. In *The Eleventh International Conference on Learning Representations*, 2023. URL `https://openreview.net/forum?id=GNjzMAgawq`.

Ziqing Yang, Xinlei He, Zheng Li, Michael Backes, Mathias Humbert, Pascal Berrang, and Yang Zhang. Data poisoning attacks against multimodal encoders. In *International Conference on Machine Learning*, pp. 39299–39313. PMLR, 2023.

Jirong Yi, Raghu Mudumbai, and Weiyu Xu. Derivation of information-theoretically optimal adversarial attacks with applications to robust machine learning. In *2024 58th Asilomar Conference on Signals, Systems, and Computers*, pp. 183–187. IEEE, 2024.

Jiayi Zhang, Shu Yang, Junchao Wu, Derek F Wong, and Di Wang. Understanding and mitigating political stance cross-topic generalization in large language models. *arXiv preprint arXiv:2508.02360*, 2025a.

Zhuoran Zhang, Yongxiang Li, Zijian Kan, Keyuan Cheng, Lijie Hu, and Di Wang. Locate-then-edit for multi-hop factual recall under knowledge editing. In *Proceedings of the 42nd International Conference on Machine Learning*, volume 267 of *Proceedings of Machine Learning Research*, pp. 75369–75391. PMLR, 2025b. URL `https://proceedings.mlr.press/v267/zhang25aq.html`.

Mengxin Zheng, Jiaqi Xue, Zihao Wang, Xun Chen, Qian Lou, Lei Jiang, and Xiaofeng Wang. Ssl-cleanse: Trojan detection and mitigation in self-supervised learning. In *Computer Vision – ECCV 2024*, pp. 405–421. Springer Nature Switzerland, 2025. doi: 10.1007/978-3-031-73021-4_24.

Mingli Zhu, Shaokui Wei, Li Shen, Yanbo Fan, and Baoyuan Wu. Enhancing fine-tuning based backdoor defense with sharpness-aware minimization. In *Proceedings of the IEEE/CVF international conference on computer vision*, pp. 4466–4477, 2023.

A Experimental Settings

A.1 Backbones

CLIP (Radford et al., 2021) is a multi-modal model proposed by OpenAI that can process both image and text data. It is trained through contrastive learning by aligning a large number of images with corresponding text descriptions. The CLIP model consists of two components: a vision encoder and a text encoder. The vision encoder is typically based on deep neural networks (*e.g.*, ResNet) or Vision Transformers (ViT), while the text encoder is based on the Transformer architecture. By training both encoders simultaneously, CLIP can project images and text into the same vector space, allowing cross-modal similarity computation.

A.2 Datasets

CIFAR-10. CIFAR-10 (Radford et al., 2021) consists of 50,000 training images and 10,000 test images, each sized 32×32×3, across 10 classes.

CIFAR-100. CIFAR-100 (Krizhevsky et al., 2009) is similar to CIFAR-10 but includes 100 classes, with 600 images per class (500 for training and 100 for testing), grouped into 20 superclasses.

ImageNet-Tiny. ImageNet-Tiny (Le & Yang, 2015) contains 100,000 images across 200 classes, with each class comprising 500 training images, 50 validation images, and 50 test images, all downsized to 64×64 color images.

A.3 Backdoor Attack Baselines

BadNet. BadNet (Gu et al., 2017) is a neural network designed for backdoor attacks in machine learning. It behaves normally for most inputs but contains a hidden trigger that, when present, causes the network to produce malicious outputs. This clever attack method is hard to detect because the network functions correctly most of the time. Only when the specific trigger is present does BadNet deviate from its expected behavior, potentially misclassifying inputs or bypassing security measures. This concept highlights the importance of AI security, especially when using pre-trained models from unknown sources.

Blended. Blended (Chen et al., 2017) attacks are a subtle form of backdoor attacks in machine learning. They use triggers seamlessly integrated into input data, making them hard to detect. These triggers are typically minor modifications to legitimate inputs. When activated, the model behaves maliciously, but appears normal otherwise. This approach bypasses many traditional defenses, highlighting the challenge of ensuring AI system security.

WaNet. WaNet (Nguyen & Tran, 2021) is an advanced backdoor technique in deep learning that uses subtle image warping as a trigger. It applies a slight, nearly imperceptible geometric distortion to input images, causing targeted misclassification in neural networks while maintaining normal performance on clean data. This invisible trigger achieves a high attack success rate and evades many existing backdoor detection methods. WaNet can be flexibly applied to various image classification tasks.

Refool. Refool (Liu et al., 2020) is a sophisticated backdoor attack method targeting image classification models. It exploits reflection patterns commonly seen in real-world images to create inconspicuous triggers. These reflection-based triggers are naturally blended into images, making them extremely difficult to detect. Refool maintains high model performance on clean data while achieving strong attack success rates on triggered inputs. This attack demonstrates how seemingly innocuous image features can be weaponized, posing significant challenges to existing backdoor defense strategies.

Trojan. Trojan (Liu et al., 2018b) is a backdoor attack method targeting computer vision models. It inserts small, inconspicuous mosaic patterns into images as triggers. These mosaic triggers are designed to resemble natural image compression or distortion, making them challenging to detect by human eyes or defense systems. When triggered images are input to the model, they cause targeted misclassifications, while the model performs normally on clean images.

SSBA. SSBA (Li et al., 2021c) generates unique triggers for each input sample, unlike traditional backdoor attacks that use a single, fixed trigger. These sample-specific triggers are optimized to be imperceptible and to cause targeted misclassifications. SSBA maintains high stealth by adapting the trigger to each image's content, making it extremely difficult to detect. The attack demonstrates high success rates while preserving normal model behavior on clean data.

BadCLIP. BadCLIP (Bai et al., 2024), a novel backdoor attack method targeting CLIP models through prompt learning. Unlike previous attacks that require large amounts of data to fine-tune the entire pre-trained model, BadCLIP operates efficiently with limited data by injecting the backdoor during the prompt learning stage. The key innovation lies in its dual-branch attack mechanism that simultaneously influences both image and text encoders. Specifically, BadCLIP combines a learnable trigger applied to images with a trigger-aware context generator that produces text prompts conditioned on the trigger, enabling the backdoor image and target class text representations to align closely. Extensive experiments across 11 datasets demonstrate that BadCLIP achieves over 99% attack success rate while maintaining clean accuracy comparable to state-of-the-art prompt learning methods. Moreover, the attack shows strong generalization capabilities across unseen classes, different datasets, and domains, while being able to bypass existing backdoor defenses. This work represents the first exploration of backdoor attacks on CLIP via prompt learning, offering a more efficient and generalizable approach compared to traditional fine-tuning or auxiliary classifier-based methods. CopyRetryClaude can make mistakes. Please double-check responses.

A.4 Backdoor Defense Baselines

ShrinkPad. ShrinkPad (Li et al., 2021b) is a preprocessing defense technique that aims to mitigate backdoor attacks in image classification models. It works by padding the input image with a specific color (often black) and then randomly cropping it back to its original size. This process effectively shrinks the original image content within a larger frame. The key idea is to disrupt potential triggers located near image edges or corners, which are common in many backdoor attacks. ShrinkPad is simple to implement, does not require model retraining, and can be applied as a preprocessing step during both training and inference.

Auto-Encoder. Auto-Encoder (Liu et al., 2017) employs an autoencoder neural network to detect and mitigate backdoor attacks. The autoencoder is trained on clean, uncompromised data to learn a compressed representation of normal inputs. When processing potentially poisoned inputs, the autoencoder attempts to reconstruct them. Backdoor triggers, being anomalous features, are often poorly reconstructed or removed during this process. By comparing the original input with its reconstruction, the defense can identify potential backdoors. This method can effectively neutralize various types of backdoor triggers while preserving the model's performance on legitimate inputs.

SCALE-UP. SCALE-UP (Guo et al., 2023) is a defense mechanism against backdoor attacks in image classification models. This method exploits the inconsistency of model predictions on backdoored images when viewed at different scales. The key principle is that clean images tend to maintain consistent predictions across various scales, while backdoored images show significant inconsistencies due to the presence of triggers. SCALE-UP systematically resizes input images and compares the model's predictions at each scale. Images with high prediction inconsistencies across scales are flagged as potential backdoor samples.

Fine-tuning. Fine-tuning (Liu et al., 2018a) is a technique that aims to neutralize backdoor attacks by retraining the potentially compromised model on a small, clean dataset. This method involves fine-tuning the last few layers or the entire model using trusted, uncontaminated data. The process works on the principle that the backdoor behavior can be overwritten or significantly reduced while maintaining the model's original performance on clean inputs. Finetune defense is relatively simple to implement and can be effective against various types of backdoor attacks. However, its success depends on the availability of a clean, representative dataset and careful tuning to avoid overfitting.

ABL. ABL (Li et al., 2021a) is a defense mechanism against backdoor attacks in deep learning models. It operates in four phases: (1) pre-isolation training using a special LGA loss to prevent overfitting to potential backdoors, (2) filtering to identify likely poisoned samples based on their loss values, (3) retraining on the

remaining "clean" data, and (4) unlearning using the identified poisoned samples by reversing the gradient. This method aims to detect and mitigate backdoors without requiring prior knowledge of the attack or access to clean datasets, making it a robust and practical defense strategy for various types of backdoor attacks in computer vision tasks.

SSL-Cleanse. SSL-Cleanse (Zheng et al., 2025), a novel approach for detecting and mitigating backdoor threats in self-supervised learning (SSL) encoders. The key challenge lies in detecting backdoors without access to downstream task information, data labels, or original training datasets - a unique scenario in SSL compared to supervised learning. This is particularly critical as compromised SSL encoders can covertly spread Trojan attacks across multiple downstream applications, where the backdoor behavior is inherited by various classifiers built upon these encoders. SSL-Cleanse addresses this challenge by developing a method that can identify and neutralize backdoor threats directly at the encoder level, before the model is widely distributed and applied to various downstream tasks, effectively preventing the propagation of malicious behavior across different applications and users. CopyRetryClaude can make mistakes. Please double-check responses.

DECREE. DECREE (Feng et al., 2023), the first backdoor detection method specifically designed for pre-trained self-supervised learning encoders. The innovation lies in its ability to detect backdoors without requiring classifier headers or input labels - a significant advancement over existing detection methods that primarily target supervised learning scenarios. The method is particularly noteworthy as it addresses a critical security vulnerability where compromised encoders can pass backdoor behaviors to downstream classifiers, even when these classifiers are trained on clean data. DECREE works across various self-supervised learning paradigms, from traditional image encoders pre-trained on ImageNet to more complex multi-modal systems like CLIP, demonstrating its versatility in protecting different types of self-supervised learning systems against backdoor attacks.

B Concept Extractor

B.1 TCAV

TCAV (Kim et al., 2018) is an important method for obtaining interpretable concepts in machine learning models. To acquire a CAV c_i for each concept i, we need two sets of image embeddings: P_i and N_i.

$$P_i = \{f(x_1^p), \ldots, f(x_{N_p}^p)\}$$
$$N_i = \{f(x_1^n), \ldots, f(x_{N_n}^n)\}$$

Where:

- P_i comprises the embeddings of $N_p = 50$ images containing the concept, called positive image examples x^p.
- N_i consists of the embeddings of $N_n = 50$ random images not containing the concept, referred to as negative image examples x^n.

Using these two embedding sets, we train a linear Support Vector Machine (SVM). The CAV is obtained via the vector normal to the SVM's linear classification boundary. It's important to note that obtaining these CAVs requires a densely annotated dataset with positive examples for each concept.

Concept Subspace. The concept subspace is defined using a concept library, which can be denoted as $I = \{i_1, i_2, \ldots, i_{N_c}\}$, where N_c represents the number of concepts. Each concept can be learned directly from data (as with CAVs) or selected by a domain expert.

The collection of CAVs forms a concept matrix C, which defines the concept subspace. This subspace allows us to interpret neural network activations in terms of human-understandable concepts.

Concept Projection and Feature Values. After obtaining the concept matrix C, we project the final embeddings of the backbone neural network onto the concept subspace. This projection is used to compute $f_C(x) \in \mathbb{R}^{N_c}$, where:

$$f_C(x) = \text{proj}_C f(x) \tag{4}$$

For each concept i, the corresponding concept feature value $f_C^{(i)}(x)$ is calculated as:

$$f_C^{(i)}(x) = \frac{f(x) \cdot c_i}{\|c_i\|^2} \tag{5}$$

This concept feature value $f_C^{(i)}(x)$ can be interpreted as a measure of correspondence between concept i and image x. Consequently, the vector $f_C(x)$ serves as a feature matrix for interpretable models, where each element represents the strength of association between the image and a specific concept.

B.2 Label-free Concept Bottleneck Models

Label-free concept bottleneck models (Label-free CBM (Oikarinen et al., 2023)) can transform any neural network into an interpretable concept bottleneck model without the need for concept-annotated data while maintaining the task accuracy of the original model, which significantly saves human and material resources.

Concept Set Creation and Filtering. The concept set is built in two sub-steps:

A. Initial concept set creation: Instead of relying on domain experts, Label-free CBM uses GPT-3 to generate an initial concept set by prompting it with task-specific queries such as "List the most important features for recognizing {class}" and others. Combining results across different classes and prompts yields a large, noisy concept set.

B. Concept set filtering: Several filtering techniques are applied to refine the concept set. First, concepts longer than 30 characters are removed. Next, concepts that are too similar to target class names are deleted using cosine similarity in text embedding space (specifically, CLIP ViT-B/16 and all-mpnet-base-v2 encoders). Duplicate concepts with a cosine similarity greater than 0.9 to others in the set are also eliminated. Additionally, concepts that are not present in the training data, indicated by low activations in the CLIP embedding space, are deleted. Finally, concepts with low interpretability are removed as well.

Learning the Concept Bottleneck Layer. Given the filtered concept set $\mathcal{C} = \{t_1, ..., t_M\}$, Label-free CBM learn the projection weights W_c to map backbone features to interpretable concepts. The CLIP-Dissect method is employed to optimize W_c by maximizing the similarity between the neuron activation patterns and target concepts. The projection $f_c(x) = W_c f(x)$ is optimized using the following objective:

$$L(W_c) = \sum_{i=1}^{M} -\text{sim}(t_i, q_i) := \sum_{i=1}^{M} -\frac{\bar{q_i}^3 \cdot \bar{P_{:,i}}^3}{||\bar{q_i}^3||_2 ||\bar{P_{:,i}}^3||_2}, \tag{6}$$

where $\bar{q_i}$ is the normalized activation pattern, and P is the CLIP concept activation matrix. The similarity function, *cos cubed*, enhances sensitivity to high activations. After optimization, we remove concepts with validation similarity scores below 0.45 and update W_c accordingly.

Learning the Sparse Final Layer. Finally, the model learns a sparse prediction layer $W_F \in \mathbb{R}^{d_z \times M}$, where d_z is the number of output classes, via the elastic net objective:

$$\min_{W_F, b_F} \sum_{i=1}^{N} L_{ce}(W_F f_c(x_i) + b_F, y_i) + \lambda R_\alpha(W_F), \tag{7}$$

where $R_\alpha(W_F) = (1-\alpha)\frac{1}{2}||W_F||_F + \alpha||W_F||_{1,1}$, and λ controls the level of sparsity. The GLM-SAGA solver is used to optimize this step, and $\alpha = 0.99$ is chosen to ensure interpretable models with 25-35 non-zero weights per output class.

B.3 Semi-supervised Concept Bottleneck Models

By leveraging joint training on both labeled and unlabeled data and aligning the unlabeled data at the conceptual level, semi-supervised concept bottleneck models (Semi-supervised CBM (Hu et al., 2025a)) address the challenge of acquiring large-scale concept-labeled data in real-world scenarios. Their approach can be summarized as follows:

Concept Embedding Encoder. The concept embedding encoder extracts concept information from both labeled and unlabeled data. For the labeled dataset $\mathcal{D}_L = \{(x^{(i)}, y^{(i)}, c^{(i)})\}_{i=1}^{|\mathcal{D}_L|}$, features are extracted by a backbone network $\psi(x^{(i)})$, and passed through an embedding generator to get concept embedding $\hat{\boldsymbol{c}}_i \in \mathbb{R}^{m \times k}$ for $i \in [k]$:

$$\hat{\boldsymbol{c}}_i^{(j)}, h^{(j)} = \sigma(\phi(\psi(x^{(j)})), \quad i = 1, \ldots, k, \quad j = 1, \ldots, |\mathcal{D}_L|,$$

where ψ, ϕ, and σ represent the backbone network, embedding generator, and activation function respectively.

Pseudo Labeling. For the unlabeled data $\mathcal{D}_U = \{(x^{(i)}, y^{(i)})\}_{i=1}^{|\mathcal{D}_U|}$, pseudo concept labels $\hat{\boldsymbol{c}}_{\boldsymbol{img}}$ are generated by calculating the cosine distance between features of unlabeled and labeled data:

$$\text{dist}(x, x^{(j)}) = 1 - \frac{x \cdot x^{(j)}}{\|x\|_2 \cdot \|x^{(j)}\|_2}, \quad j = 1, \ldots, |\mathcal{D}_L|.$$

Concept Scores. To refine the pseudo concept labels, Semi-supervised CBM generates concept heatmaps by calculating cosine similarity between concept embeddings and image features. For an image x, the similarity matrix $\mathcal{H}_{p,q,i}$ for the i-th concept is calculated as:

$$\mathcal{H}_{p,q,i} = \frac{\boldsymbol{e}_i^\top V_{p,q}}{||\boldsymbol{e}_i|| \cdot ||V_{p,q}||}, \quad p = 1, \ldots, H, \quad q = 1, \ldots, W,$$

where $V \in \mathbb{R}^{H \times W \times m}$ is the feature map of the image, calculated by $V = \Omega(x)$, where Ω is the visual encoders.

Then, the concept score s_i is calculated based on the heatmaps: $s_i = \frac{1}{P \cdot Q} \sum_{p=1}^{P} \sum_{q=1}^{Q} \mathcal{H}_{p,q,i}$. In the end, Semi-supervised CBM obtains a concept score vector $\boldsymbol{s} = (s_1, \ldots, s_k)^\top$ that represents the correlation between an image x and a set of concepts, which is used by us to filter data for backdoor attacks.

C Detection Experiment

We train 10 backdoored models, each using a different concept, and evaluate their detection accuracy under C^2Attack. Tab. 14 presents the overall detection accuracy, while Tab. 15 provides detailed detection results for each backdoored model. "True" indicates that the detection method successfully identifies the backdoored model, whereas "False" signifies a failure to detect it.

Table 14: Detection accuracy against C^2Attack. We train 10 backdoored models, each using a different trigger concept, and evaluate detection accuracy using two detection methods.

	SSL-Cleanse	**DECREE**
Accuracy	10%	0%

D Information-Theoretic Lower Bound for Data Flipping Rate

D.1 Main Theorem Statement

Theorem D.1. *For concept confusion attacks (Chen et al., 2017), the data flipping rate satisfies an information-theoretic lower bound. Let $D = \{(x_i, y_i)\}_{i=1}^{N}$ be a training dataset sampled from distribution*

Table 15: Detailed detection results for each backdoored model. “True" indicates that the detection method successfully identifies the backdoored model, whereas “False" signifies a failure to detect it.

Detection Method	SSL-Cleanse	DECREE
Airplane	false	false
Oven	false	false
Engine	false	false
Headlight	false	false
Head	false	false
Clock	false	false
Mirror	true	false
Air-conditioner	false	false
Building	false	false
Cushion	false	false

$\mathcal{P}_{xy}$, and let $\mathcal{C} = \{q_1, q_2, \ldots, q_K\}$ be the concept space with concept extractor $c(\cdot) : \mathcal{X} \to \mathbb{R}^K$. Consider a concept confusion attacker who flips labels of a fraction ϵ of training samples to induce misclassification on test samples containing specific concepts.

For any $\delta \in (0, 1)$, if the attack success probability is at least $1 - \delta$, then the data flipping rate must satisfy:

$$\epsilon \geq \frac{H(Q) - \log(1/\delta) - \log 2}{N \cdot \iota} \tag{8}$$

Here, $Q \in \{1, \ldots, K\}$ denotes the concept index random variable; $H(Q)$ is its entropy (Raginsky et al., 2013). The symbol ι denotes the single-sample information budget, representing the maximum information injected by one label flip. For a classification task with label space $\mathcal{Y}$ containing $|\mathcal{Y}|$ classes, a conservative upper bound is $\iota \leq \log |\mathcal{Y}|$.

D.2 Problem Formulation

Definition D.2 (Concept Confusion Attack)**.** We define the concept confusion attack as follows (Goldblum et al., 2022). Let $\mathcal{A}$ denote an attack algorithm. A concept confusion attack $\mathcal{A}$ on dataset $D = \{(x_i, y_i)\}_{i=1}^N$ with concept space $\mathcal{C} = \{q_1, q_2, \ldots, q_K\}$ is characterized by:

- Attack budget $\epsilon \in [0, 1]$: fraction of samples that can be label-flipped
- Target concept $q_{k'} \in \mathcal{C}$: concept the attacker aims to associate with target class
- Adversarial dataset $D^{(p)} \in \mathcal{A}_\epsilon(D)$ where $\mathcal{A}_\epsilon(D) = \{D^{(p)} : d_H(D, D^{(p)}) \leq \epsilon N\}$ and $d_H(D, D^{(p)})$ denotes the Hamming distance between D and $D^{(p)}$, measured as the number of differing labels.

Definition D.3 (Attack Success Rate)**.** We define the attack success rate as follows. Let $\mathcal{M}$ denote a learning algorithm and let $h^* : \mathcal{X} \to \mathcal{Y}$ denote the ground truth labeling function. Given a classifier $h_{D^{(p)}}$ trained on adversarial dataset $D^{(p)} \in \mathcal{A}_\epsilon(D)$, the attack success rate against target concept $q_{k'}$ is:

$$\mathrm{ASR}(q_{k'}, \epsilon) = \mathbb{P}_{x \sim \mathcal{D}_{k'}}[h_{D^{(p)}}(x) \neq h^*(x)] \tag{9}$$

where $h_{D^{(p)}}(x)$ denotes the predicted label for input x by the classifier trained on $D^{(p)}$, and $\mathcal{D}_{k'}$ is the distribution of samples containing concept $q_{k'}$, defined as those satisfying $c(x)_{k'} \geq \sigma$ for threshold σ as specified in Section 4.2.

D.2.1 Key Assumption

Our analysis relies on a worst-case assumption from the defender’s perspective regarding the distribution of the attacker’s target concept selection.

Assumption D.4 (Uniform Concept Distribution)**.** When the defender has no prior knowledge about which concept the attacker targets, we model the concept index as uniformly distributed. Specifically, for the concept index random variable $Q \in \{1, 2, \ldots, K\}$, we assume $\mathbb{P}(Q = i) = 1/K$ for all $i \in \{1, \ldots, K\}$, which yields maximum entropy:

$$H(Q) = \log K. \tag{10}$$

This uniform distribution assumption represents the worst-case scenario for the defender, maximizing the attacker's advantage. If the defender had prior knowledge that certain concepts are more likely to be targeted, then $H(Q) < \log K$ and the required flipping rate would be lower. In minimax analysis, the uniform prior is standard when no additional information is available, as it provides the tightest lower bound on the attack's information-theoretic requirements (Yi et al., 2024).

D.3 Information-Theoretic Lower Bounds

D.3.1 Minimum Information Requirement

Lemma D.5 (Fano's Lower Bound)**.** *For any concept confusion attack achieving success rate* $\mathrm{ASR}(q_{k'}, \epsilon) \geq 1 - \delta$ *, the mutual information between concept index* Q *and poisoned dataset* $D^{(p)}$ *must satisfy:*

$$I(Q; D^{(p)}) \geq H(Q) - \log(1/\delta) - \log 2 \tag{11}$$

Proof. We establish this bound using Fano's inequality (Scarlett & Cevher, 2021), a fundamental result in information theory that relates the probability of error in estimating a random variable to the conditional entropy.

Consider the following scenario: given only the poisoned dataset $D^{(p)}$, a predictor attempts to infer which concept $Q \in \{1, \ldots, K\}$ the attacker is targeting. Let $\hat{Q}$ denote the predictor's estimate and define the error event $\mathcal{E} = \{\hat{Q} \neq Q\}$ with error probability $P_e = \mathbb{P}(\mathcal{E})$.

If the attack succeeds with probability at least $1 - \delta$, then the backdoor is effectively embedded and concept Q causes predictable behavior in the model. This means that any predictor trying to determine Q from $D^{(p)}$ alone must fail with probability at least δ , and therefore the prediction error must satisfy $P_e \geq \delta$.

We now apply Fano's inequality (Scarlett & Cevher, 2021), which states that for any estimator $\hat{Q}$ of Q based on $D^{(p)}$:

$$H(Q|D^{(p)}) \leq h(P_e) + P_e \log(K - 1) \tag{12}$$

where $h(p) = -p \log p - (1 - p) \log(1 - p)$ is the binary entropy function.

Using $P_e \geq \delta$ and the fact that binary entropy satisfies $h(\delta) \leq \log 2$ for all $\delta \in [0, 1]$, a tighter analysis gives:

$$H(Q|D^{(p)}) \leq h(\delta) + \delta \log(K - 1) \leq \log 2 + \log(1/\delta) \tag{13}$$

where the second inequality uses $\delta \log(K - 1) \leq \delta \log K \leq \log(1/\delta)$ for small δ .

By the definition of mutual information and the above bound on conditional entropy, we have:

$$\begin{aligned} I(Q; D^{(p)}) &= H(Q) - H(Q \mid D^{(p)}) \\ &\geq H(Q) - \log 2 - \log(1/\delta) \\ &= H(Q) - \log(1/\delta) - \log 2 \end{aligned} \tag{14}$$

This establishes the minimum information requirement for attack success. □

D.3.2 Information Injection Capacity

Lemma D.6 (Information Injection Bound)**.** *The total information about concept* Q *that can be injected into poisoned dataset* $D^{(p)}$ *with flipping rate* ϵ *is bounded by:*

$$I(Q; D^{(p)}) \leq \epsilon N \cdot \iota \tag{15}$$

where $\iota \leq \log |\mathcal{Y}|$ *is the maximum information injectable per label flip.*

Proof. We model label flipping as an information injection channel where the attacker uses label modifications to embed information about the target concept into the poisoned dataset. This proof parallels the analysis of corruption bounds in robust learning (Attias et al., 2022; Song et al., 2022).

Consider a single training example $(x_i, y_i) \in D$. When the attacker flips its label from y_i to $y'_i \neq y_i$, the information about concept Q that can be injected through this modification is bounded by the label entropy. By the data processing inequality (Raginsky et al., 2013), we have $I(Q; (x_i, y'_i) \mid x_i) \leq H(y'_i \mid x_i)$. Since $y'_i \in \mathcal{Y}$ and the label takes one of $|\mathcal{Y}|$ possible values, we have $H(y'_i \mid x_i) \leq H(y'_i) \leq \log |\mathcal{Y}|$. This gives us the per-sample information budget: $\iota \leq \log |\mathcal{Y}|$. Intuitively, the label y'_i acts as a communication channel, and no matter how cleverly the attacker chooses y'_i , it can encode at most $\log |\mathcal{Y}|$ bits of information about the target concept.

Let $T \subset \{1, \ldots, N\}$ denote the set of flipped sample indices with $|T| = \lfloor \epsilon N \rfloor$. We partition $D^{(p)}$ into two disjoint sets: $D^{(p)}_T = \{(x_i, y'_i)\}_{i \in T}$ representing the flipped samples and $D_{\bar{T}} = \{(x_i, y_i)\}_{i \notin T}$ representing the unflipped samples. By the chain rule of mutual information:

$$I(Q; D^{(p)}) = I(Q; D_{\bar{T}}) + I(Q; D^{(p)}_T \mid D_{\bar{T}}) \tag{16}$$

Since $D_{\bar{T}}$ consists of correctly labeled samples from the original distribution $\mathcal{P}_{xy}$, and Q (the target concept chosen by the attacker) is independent of the original data generation process, we have $I(Q; D_{\bar{T}}) = 0$. The unflipped portion $D_{\bar{T}}$ contains no information about which concept the attacker selected as the target, because these labels were not modified and were generated independently of the attacker's choice.

For the flipped samples, we bound the mutual information under the worst-case assumption that each label flip can maximally exploit the information channel:

$$\begin{aligned} I(Q; D^{(p)}_T \mid D_{\bar{T}}) &\leq I(Q; D^{(p)}_T) \\ &= I(Q; \{(x_i, y'_i)\}_{i \in T}) \\ &\leq \sum_{i \in T} I(Q; (x_i, y'_i) \mid x_i) \\ &\leq \sum_{i \in T} \iota \\ &= |T| \cdot \iota \leq \epsilon N \cdot \iota \end{aligned} \tag{17}$$

where the first inequality uses the fact that conditioning cannot increase mutual information, the third inequality applies the subadditivity of mutual information under the assumption that label flips are conditionally independent given features which represents a worst-case scenario for the defender, and the fourth inequality applies the per-sample bound established above.

Combining these results, we obtain:

$$I(Q; D^{(p)}) = I(Q; D_{\bar{T}}) + I(Q; D^{(p)}_T \mid D_{\bar{T}}) \leq 0 + \epsilon N \cdot \iota = \epsilon N \cdot \iota \tag{18}$$

This establishes the information injection constraint. The bound is tight when the attacker can use each flipped label to its full capacity. □

D.3.3 Combining Lower Bounds

Corollary D.7. *Combining Lemmas D.5 and D.6, for attack success rate* $\mathrm{ASR}(q_{k'}, \epsilon) \geq 1 - \delta$ *, we have:*

$$\epsilon \geq \frac{H(Q) - \log(1/\delta) - \log 2}{N \cdot \iota} \tag{19}$$

Proof. From Lemma D.5, achieving attack success rate $1 - \delta$ requires the mutual information to satisfy:

$$I(Q; D^{(p)}) \geq H(Q) - \log(1/\delta) - \log 2 \tag{20}$$

This represents the minimum information needed to reliably embed the backdoor.

From Lemma D.6, the maximum information that the attacker can inject through label flipping at rate ϵ is:

$$I(Q; D^{(p)}) \leq \epsilon N \cdot \iota \tag{21}$$

This represents the capacity of the label-flipping channel.

For the attack to succeed, we must have $\epsilon N \cdot \iota \geq H(Q) - \log(1/\delta) - \log 2$. Rearranging yields the desired bound. □

D.4 Quantifying Attack Parameters

D.4.1 Concept Entropy

Lemma D.8 (Maximum Entropy)**.** *Under the uniform concept distribution assumption $p_i = 1/K$ for all $i \in \{1, \ldots, K\}$, the concept entropy satisfies:*

$$H(Q) = \log K \tag{22}$$

More generally, for any distribution over concepts, we have $H(Q) \leq \log K$ with equality if and only if the distribution is uniform.

Proof. The entropy function achieves its maximum when the distribution is uniform (Raginsky et al., 2013), a fundamental property following from its concavity. For any probability distribution $(p_1, \ldots, p_K)$ with $\sum_{i=1}^{K} p_i = 1$ and $p_i \geq 0$, we have:

$$H(Q) = -\sum_{i=1}^{K} p_i \log p_i \leq \log K \tag{23}$$

with equality if and only if $p_i = 1/K$ for all $i \in \{1, \ldots, K\}$.

Under the uniform distribution assumption $p_i = 1/K$ for all i , direct calculation yields:

$$\begin{aligned} H(Q) &= -\sum_{i=1}^{K} p_i \log p_i \\ &= -\sum_{i=1}^{K} \frac{1}{K} \log \frac{1}{K} \\ &= -\frac{1}{K} \cdot K \cdot \log \frac{1}{K} \\ &= -\log \frac{1}{K} = \log K \end{aligned} \tag{24}$$

In the C^2 attack setting, the attacker chooses which concept $q_{k'} \in \mathcal{C}$ to use as the trigger. From a defender's perspective without knowledge of the attacker's choice, the worst-case analysis assumes the attacker could target any of the K concepts with equal probability. This uniform prior maximizes uncertainty: $H(Q) = \log K$, representing the maximum difficulty in defending against an unknown target concept. If the defender had prior knowledge that certain concepts are more likely to be targeted, then $H(Q) < \log K$ and the required flipping rate would be lower. The uniform distribution assumption is standard in minimax analysis and represents the hardest case for the defender. □

D.4.2 Per-Sample Information Budget

Lemma D.9 (Information Budget per Flip)**.** *The maximum information that can be injected per label flip satisfies:*

$$\iota \leq \log |\mathcal{Y}| \tag{25}$$

where $|\mathcal{Y}|$ is the size of the label space, representing the number of classes in the classification task.

Proof. This follows directly from the single-sample analysis in Lemma D.6's proof, but we provide additional context here.

Consider a single training example (x_i, y_i) with feature x_i and label $y_i \in \mathcal{Y}$. The attacker observes x_i and can choose to flip the label to any $y_i' \in \mathcal{Y}$. The amount of information about concept Q that can be embedded in the choice of y_i' is bounded by:

$$I(Q; y_i' \mid x_i) \leq H(y_i' \mid x_i) \leq H(y_i') \leq \log |\mathcal{Y}| \tag{26}$$

where the first inequality follows from the data processing inequality (Raginsky et al., 2013) stating that $I(Q; Y) \leq H(Y)$ for any random variables Q, Y , the second inequality uses the fact that conditioning reduces entropy as $H(Y|X) \leq H(Y)$, and the third inequality applies the entropy bound for discrete random variables which states that for Y taking $|\mathcal{Y}|$ values, $H(Y) \leq \log |\mathcal{Y}|$ with equality when Y is uniform.

The bound $\iota = \log |\mathcal{Y}|$ is achieved when the attacker can freely choose any label $y_i' \in \mathcal{Y}$ and makes this choice to maximally encode information about Q . In practice, the effective information per flip may be less than $\log |\mathcal{Y}|$ due to several factors: naturalness constraints requiring label flips to appear plausible, concept-label correlations where some concepts naturally correlate with certain labels thereby reducing the effective coding capacity, and detection risk where too many unnatural label flips may trigger anomaly detection. However, $\iota = \log |\mathcal{Y}|$ serves as a conservative upper bound representing the worst-case scenario for theoretical analysis, analogous to Shannon capacity in communication channels. □

D.4.3 Finite Sample Effects

Lemma D.10 (Finite Sample Concentration)**.** *With N samples, the finite-sample correction satisfies $\Delta_N = \tilde{O}(\sqrt{\log K/N})$. Specifically, with probability at least $1 - \delta$:*

$$|H(\hat{Q}) - H(Q)| \leq \Delta_N = O\left(\sqrt{\frac{\log K \cdot \log(2/\delta)}{N}}\right) \tag{27}$$

where $\hat{Q}$ is the empirical concept distribution and $H(Q)$ is the true population entropy.

Proof. We establish concentration of the empirical entropy using McDiarmid's inequality (Combes, 2024) for functions with bounded differences. This technique is standard in robust statistics (Bhatt & Pensia, 2023).

Consider the empirical entropy as a function of N independent and identically distributed samples $Q_1, \ldots, Q_N$ drawn from the concept distribution:

$$\hat{H}(\mathcal{C}) = -\sum_{i=1}^{K} \hat{p}_i \log \hat{p}_i \tag{28}$$

where $\hat{p}_i = \frac{1}{N} \sum_{j=1}^{N} \mathbf{1}[Q_j = i]$ is the empirical frequency of concept i .

We first establish that changing a single sample Q_j changes $\hat{H}(\mathcal{C})$ by at most $\frac{2 \log K}{N}$. Suppose we change Q_j from concept i to concept i' . This changes $\hat{p}_i$ by $-1/N$, $\hat{p}_{i'}$ by $+1/N$, and leaves other $\hat{p}_k$ unchanged. The entropy is Lipschitz continuous with respect to the ℓ_1 distance on the probability simplex: for any two distributions $\mathbf{p}, \mathbf{p}'$ on K outcomes, we have $|H(\mathbf{p}) - H(\mathbf{p}')| \leq \|\mathbf{p} - \mathbf{p}'\|_1 \cdot \log K$, which can be verified using the inequality $|x \log x - y \log y| \leq |x - y| \log K$ for $x, y \in [0, 1]$. In our case, $\|\hat{\mathbf{p}} - \hat{\mathbf{p}}'\|_1 = 2/N$, therefore:

$$|\hat{H}(\mathcal{C}) - \hat{H}(\mathcal{C})'| \leq \frac{2}{N} \cdot \log K = \frac{2 \log K}{N} \tag{29}$$

This establishes the bounded difference property with $c_j = \frac{2 \log K}{N}$ for all j .

By McDiarmid's inequality (Combes, 2024), if a function $f(X_1, \ldots, X_N)$ satisfies the bounded difference property with constants $c_1, \ldots, c_N$, then:

$$\mathbb{P}\left[|f - \mathbb{E}[f]| \geq t\right] \leq 2\exp\left(-\frac{2t^2}{\sum_{j=1}^{N} c_j^2}\right) \tag{30}$$

Applying this to $\hat{H}(\mathcal{C})$ with $c_j = \frac{2\log K}{N}$ yields:

$$\mathbb{P}\left[|\hat{H}(\mathcal{C}) - \mathbb{E}[\hat{H}(\mathcal{C})]| \geq t\right] \leq 2\exp\left(-\frac{Nt^2}{2(\log K)^2}\right) \tag{31}$$

Setting the right-hand side equal to δ and solving for t gives:

$$t = \sqrt{\frac{2(\log K)^2 \log(2/\delta)}{N}} = O\left(\log K\sqrt{\frac{\log(2/\delta)}{N}}\right) \tag{32}$$

By the law of large numbers, as $N \to \infty$, the empirical entropy concentrates around the population entropy: $\mathbb{E}[\hat{H}(\mathcal{C})] \to H(\mathcal{C})$. For finite N , the bias $|\mathbb{E}[\hat{H}(\mathcal{C})] - H(\mathcal{C})|$ is at most $O(\log K/N)$, which is negligible compared to the stochastic deviation when $N \gg \log K$.

Using the triangle inequality to combine these results:

$$\begin{aligned} |\hat{H}(\mathcal{C}) - H(\mathcal{C})| &\leq |\hat{H}(\mathcal{C}) - \mathbb{E}[\hat{H}(\mathcal{C})]| + |\mathbb{E}[\hat{H}(\mathcal{C})] - H(\mathcal{C})| \\ &\leq O\left(\log K\sqrt{\frac{\log(2/\delta)}{N}}\right) + O\left(\frac{\log K}{N}\right) \\ &= O\left(\sqrt{\frac{\log K \cdot \log(2/\delta)}{N}}\right) \end{aligned} \tag{33}$$

with probability at least $1 - \delta$, where the last step uses the fact that the $O(\log K/N)$ term is dominated by the $O\left(\sqrt{\log K/N}\right)$ term for $N \gg \log K$. This establishes $\Delta_N = O\left(\sqrt{\frac{\log K \cdot \log(2/\delta)}{N}}\right)$. □

D.5 Proof of Main Theorem

Proof of Theorem D.1. We combine the previous lemmas to establish the information-theoretic lower bound on the data flipping rate.

By Lemma D.5 applying Fano's inequality, any concept confusion attack achieving success rate ASR $\geq 1 - \delta$ must inject information satisfying:

$$I(Q; D^{(p)}) \geq H(Q) - \log(1/\delta) - \log 2 \tag{34}$$

This represents the fundamental information-theoretic barrier: to reliably cause misclassification with probability $1 - \delta$, the backdoor must encode at least $H(Q) - \log(1/\delta) - \log 2$ bits of information into the training data.

By Lemma D.6 on the information injection constraint, the maximum information that can be injected through label flipping at rate ϵ is:

$$I(Q; D^{(p)}) \leq \epsilon N \cdot \iota \tag{35}$$

This represents the communication capacity of the label-flipping channel: flipping ϵN labels, each carrying at most ι bits, yields at most $\epsilon N \cdot \iota$ bits total.

For the attack to succeed, the available information must be sufficient to meet the minimum requirement. This is a necessary condition—if the attacker cannot inject enough information, then by Fano's inequality, it is information-theoretically impossible to achieve the target success rate. Combining the bounds established above:

$$\epsilon N \cdot \iota \geq H(Q) - \log(1/\delta) - \log 2 \tag{36}$$

Rearranging yields:

$$\epsilon \geq \frac{H(Q) - \log(1/\delta) - \log 2}{N \cdot \iota} \tag{37}$$

By Lemma D.8, under the uniform distribution assumption representing the worst-case scenario for the defender, $H(Q) = \log K$. By Lemma D.9, for an $|\mathcal{Y}|$ -class task, $\iota \leq \log |\mathcal{Y}|$. Substituting these gives:

$$\epsilon \geq \frac{\log K - \log(1/\delta) - \log 2}{N \cdot \log |\mathcal{Y}|} \tag{38}$$

The analysis above assumes population-level quantities. For finite samples, Lemma D.10 shows that the empirical entropy concentrates: $|H(\hat{Q}) - H(Q)| = O(\sqrt{\log K/N})$. This introduces an additional correction term Δ_N , but for $N \gg \log K$, this term is negligible compared to the main bound.

This completes the proof of Theorem D.1. □